Extragalactic Distance Scale lect. III

Grzegorz Pietrzyński CAMK
pietrzyn@camk.edu.pl

Photometric multicolor data:

1) age, distance
2) Reddening
3) Metallicity
4) Gravity
5) Effective temperature
6) Surface brightness (angular diameter)

T_{eff} from color

di Benedetto 1998, Alonso et al. 2999, Houdashelt et al. 2000, Ramirez & Melendez 2005, Masana et al. 2006, Gonzalez Bonofacio 2009, Casagrande et al. 2010, Wothey & Lee 2011

V-I or V-K => T_{eff}

Precision below 1 %

Strömgren filters uvby - indexes:

b-y sensitive to T_{eff} via Paschen continuum
c_1= (u-v) − (v-b) sensitive to gravity (Balmer jump)
m_1=(v-b) − (b-y) metallicity (line blanketing)

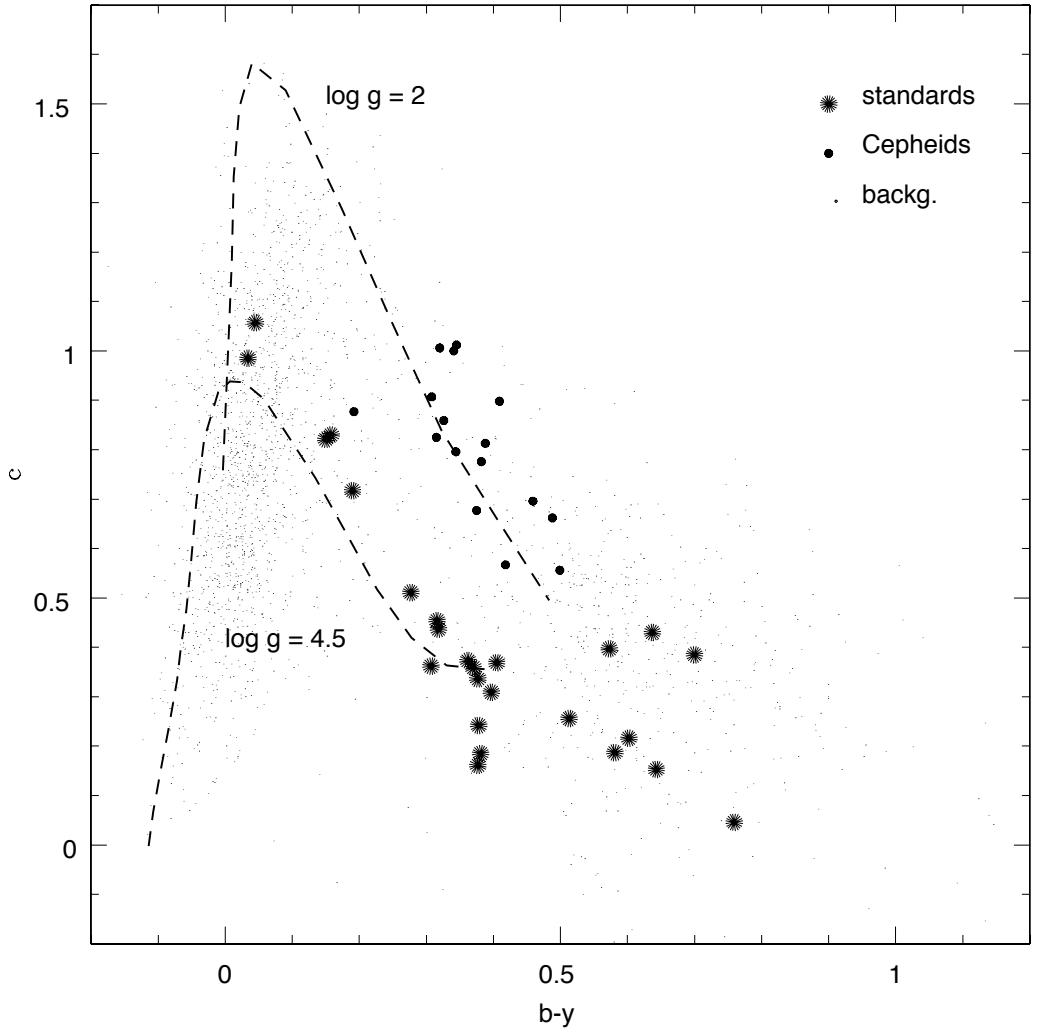

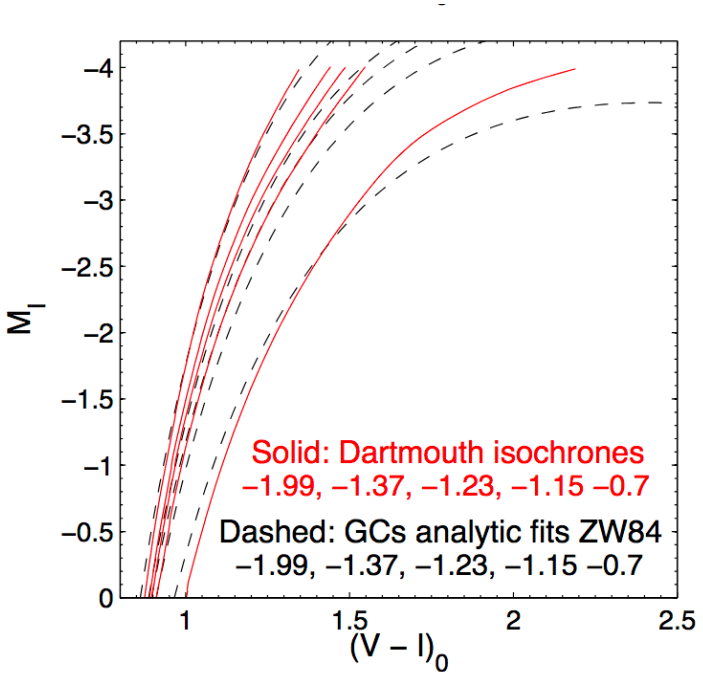
Solid: Dartmouth isochrones
−1.99, −1.37, −1.23, −1.15 −0.7
Dashed: GCs analytic fits ZW84
−1.99, −1.37, −1.23, −1.15 −0.7
M_I
$(V-I)_0$

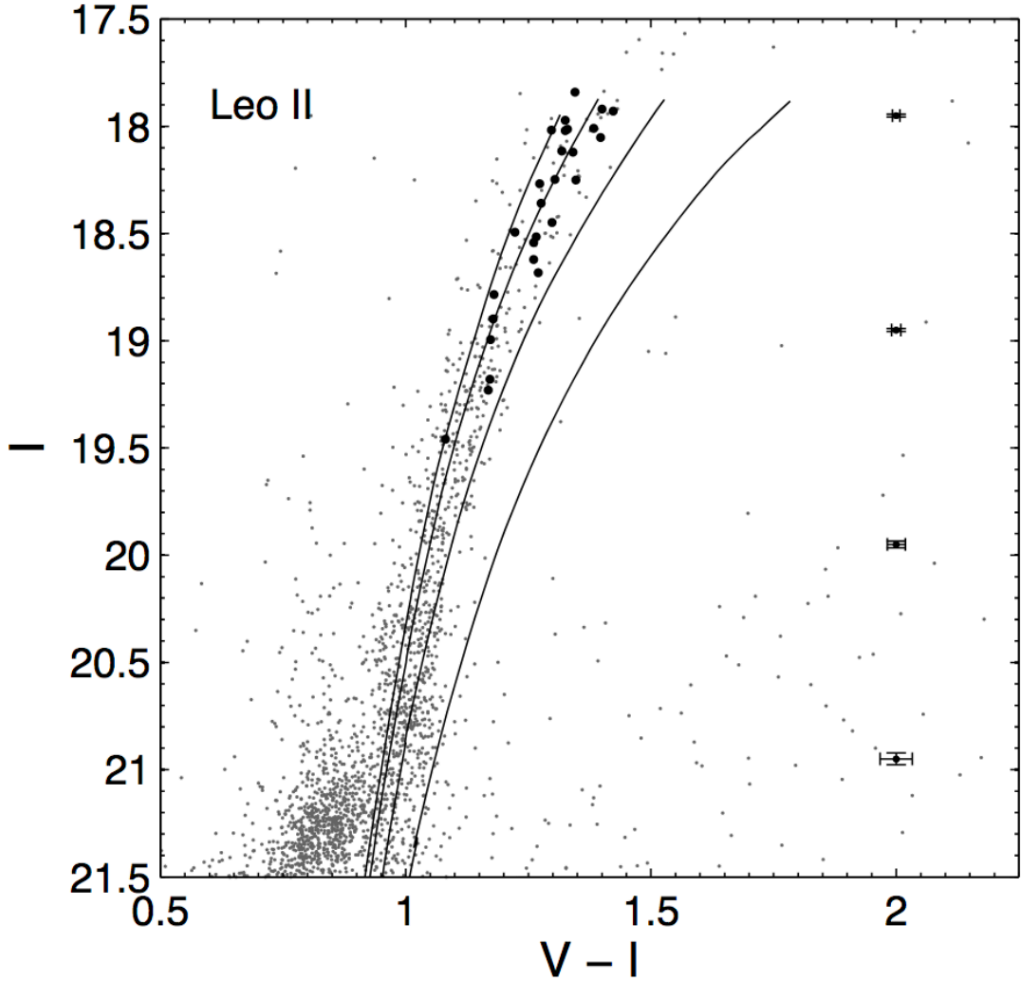
Leo II
I
V − I

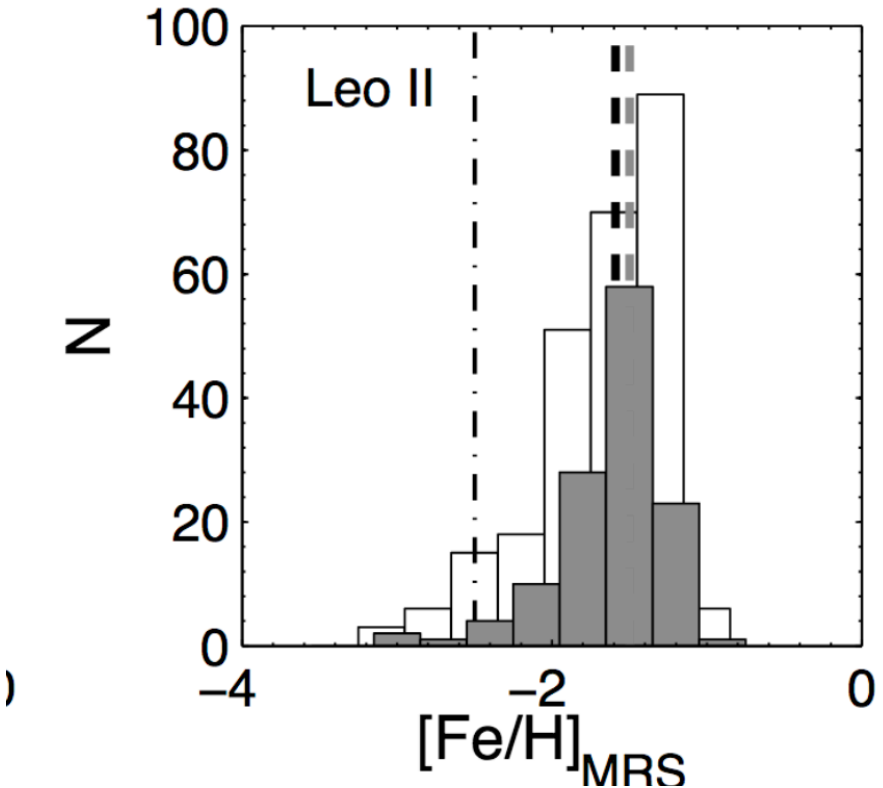
Leo II
N
$[Fe/H]_{MRS}$

SBCR

$$S_V = 2.656 + 1.483 \times (V-K)_0 - 0.044 \times (V-K)_0^2$$

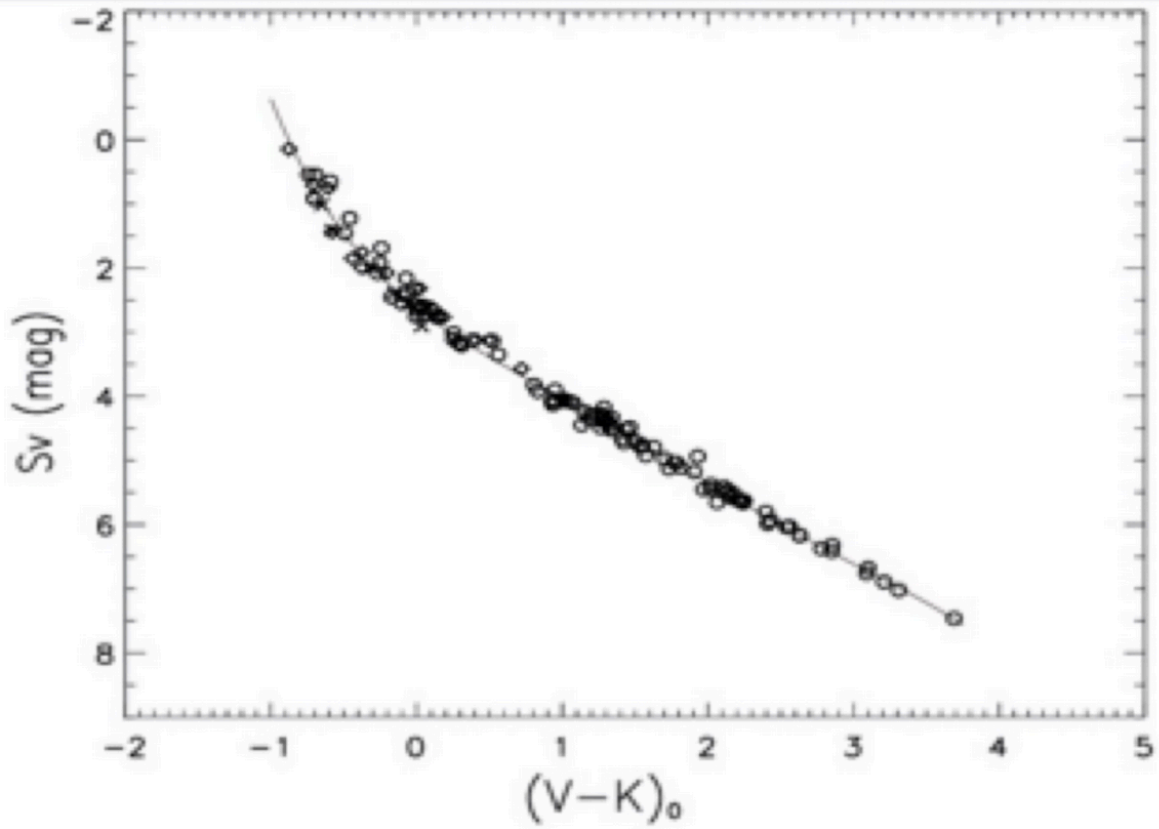

$$\phi\ [\mathrm{mas}] = 10^{0.2 \cdot (S - m_0)}$$

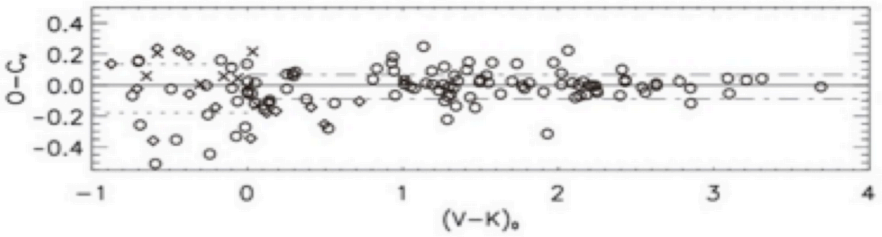

10%

2%

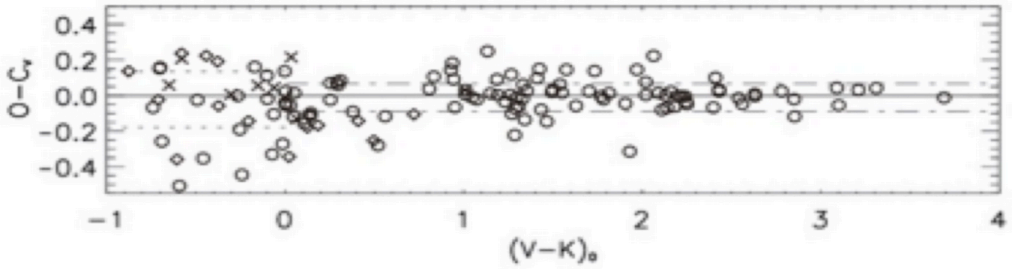

Data from 1960s

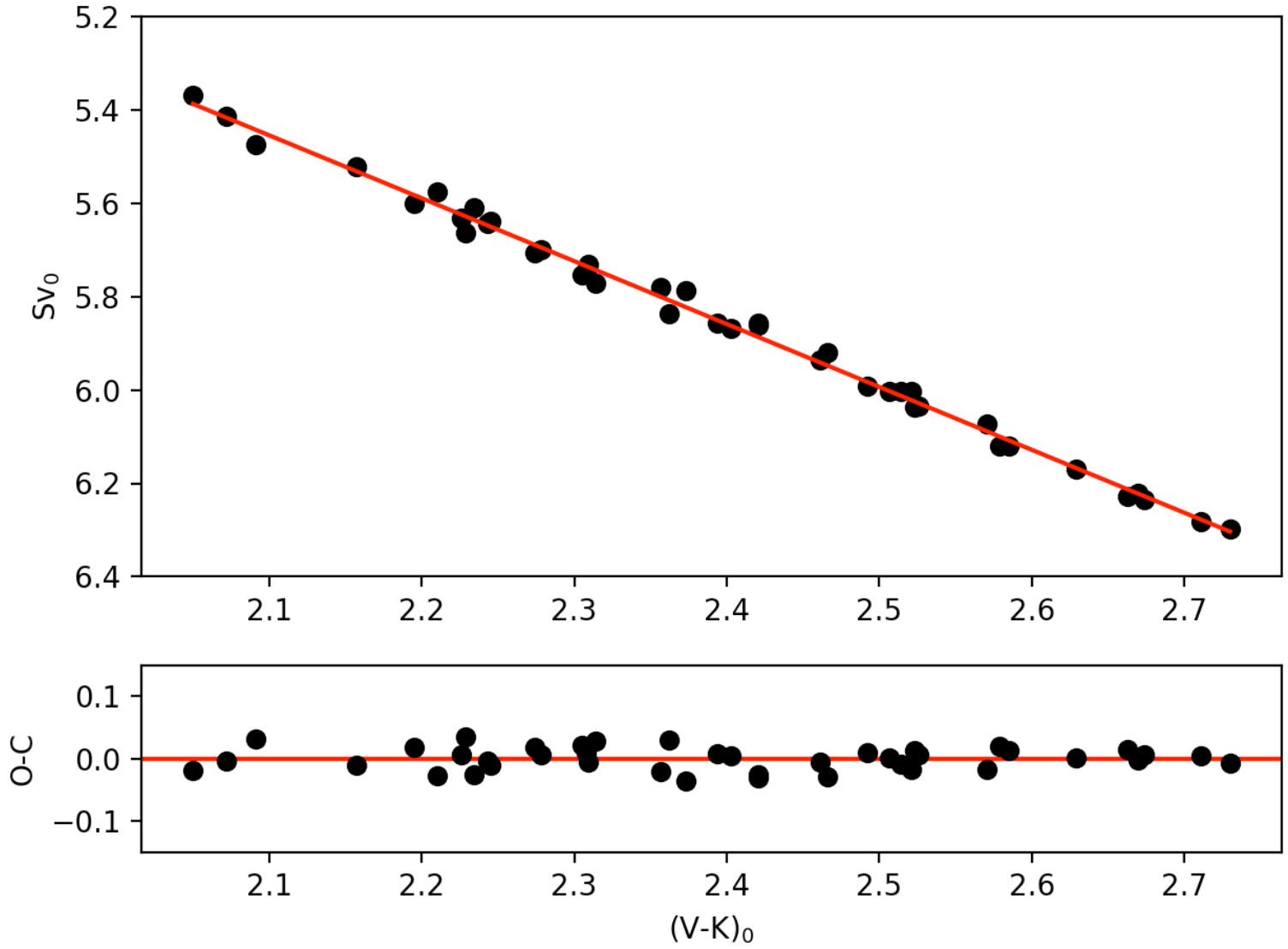

$$S_v = 1.330(\pm 0.017) \times [(V\text{-}K)_0 - 2.405] + 5.869(\pm 0.003) \text{ mag}$$

r.m.s. 0.018 mag (0.8% in angular diam.)

Reddening

$$E(B\text{-}V) = (B\text{-}V)_{observed} - (B\text{-}V)_{intrinsic}$$

Assuming extinction law => A_λ

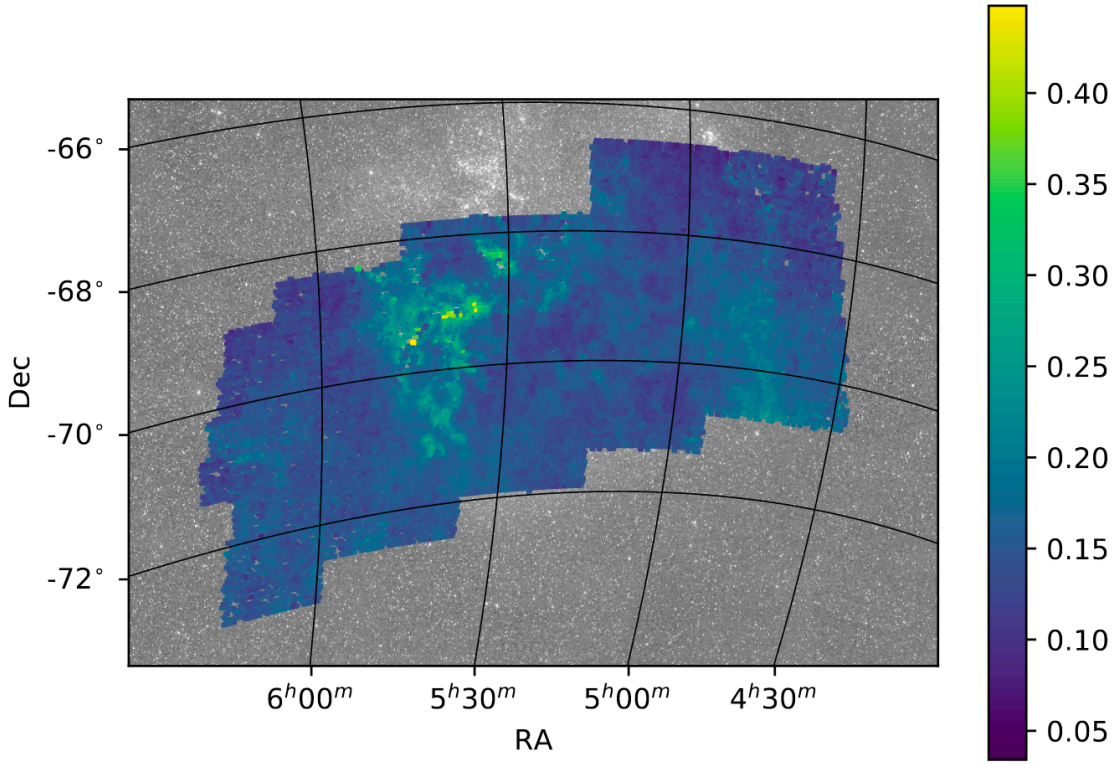

Górski et al. 2020

IR astronomy overview

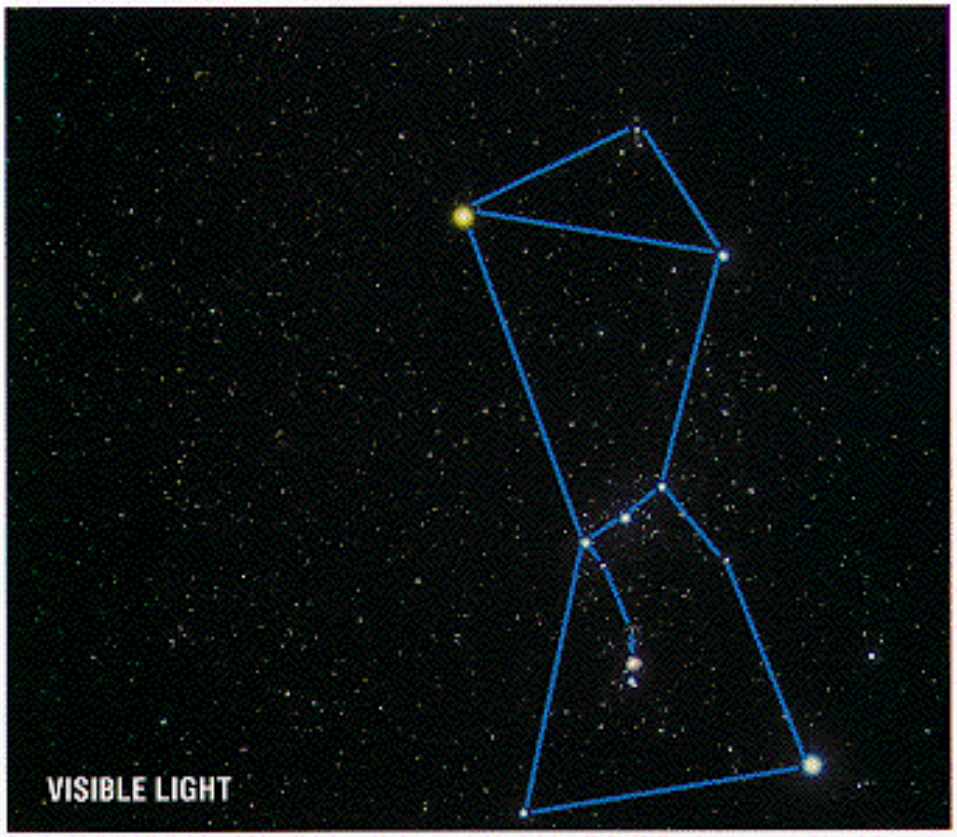

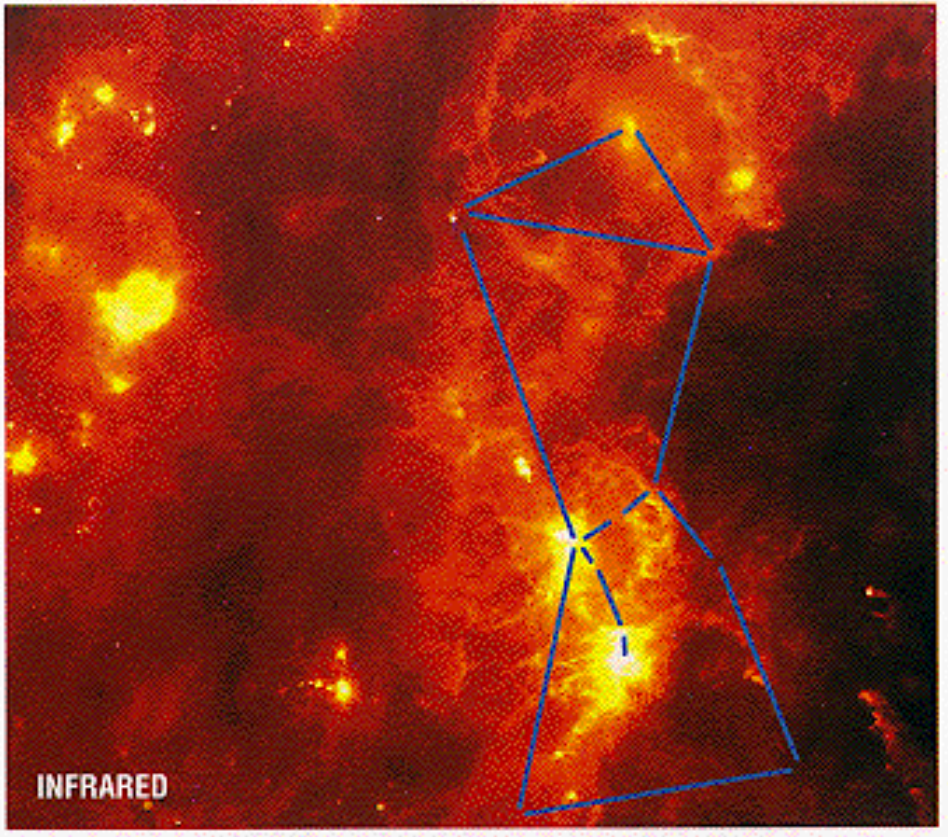

Discovery of IR

Herschel thought that the colors themselves might contain different levels of heat, so he devised a clever experiment to investigate his hypothesis.

Herschel performed further experiments on what he called the "calorific rays" that existed beyond the red part of the spectrum and found that they were reflected, refracted, absorbed and transmitted just like visible light.

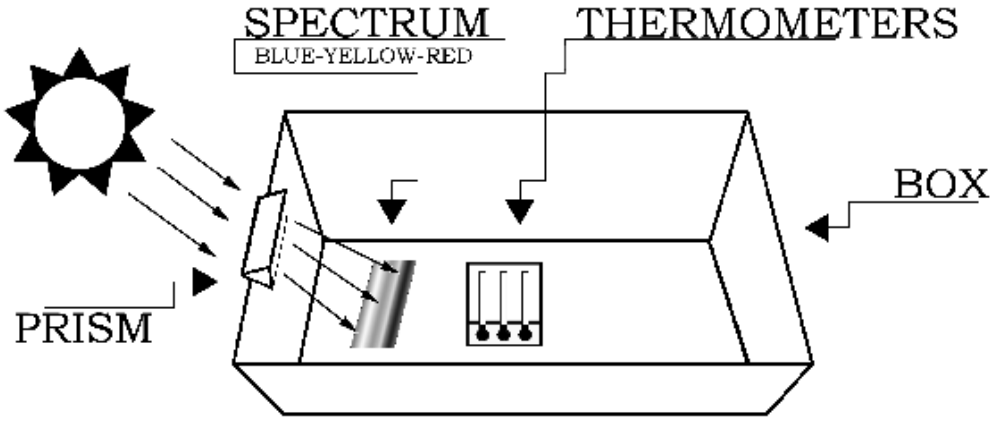

Applications

2) Health and Safety (Environmental Monitoring, Medicine, Fire Fighting, Search and rescue, Military etc)

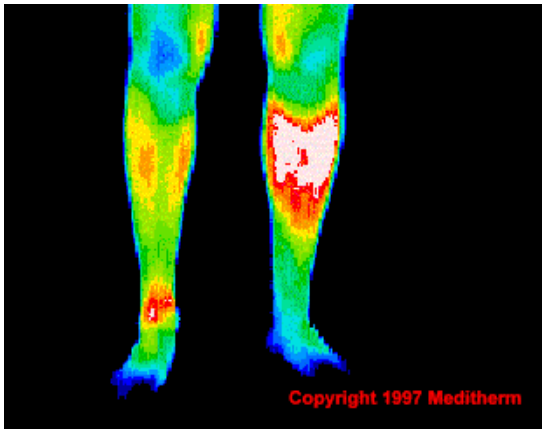

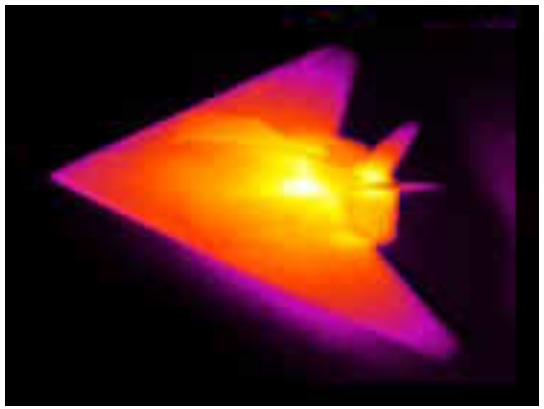

Applications

3) Commercial (Mechanical maintenance, Electrical inspections, Detecting Heat Loss, Navigations)

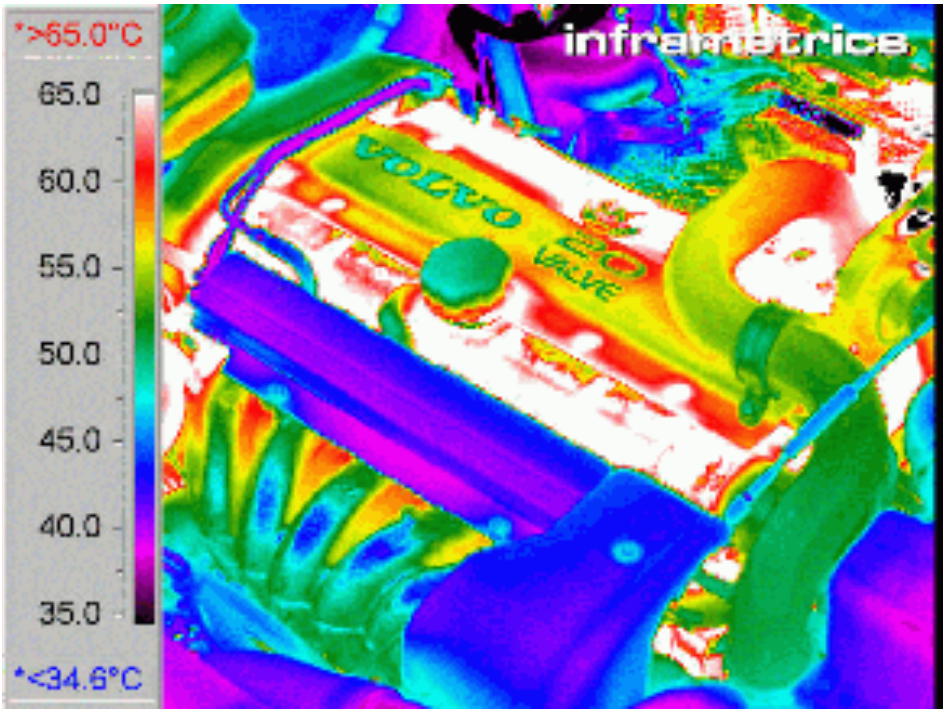

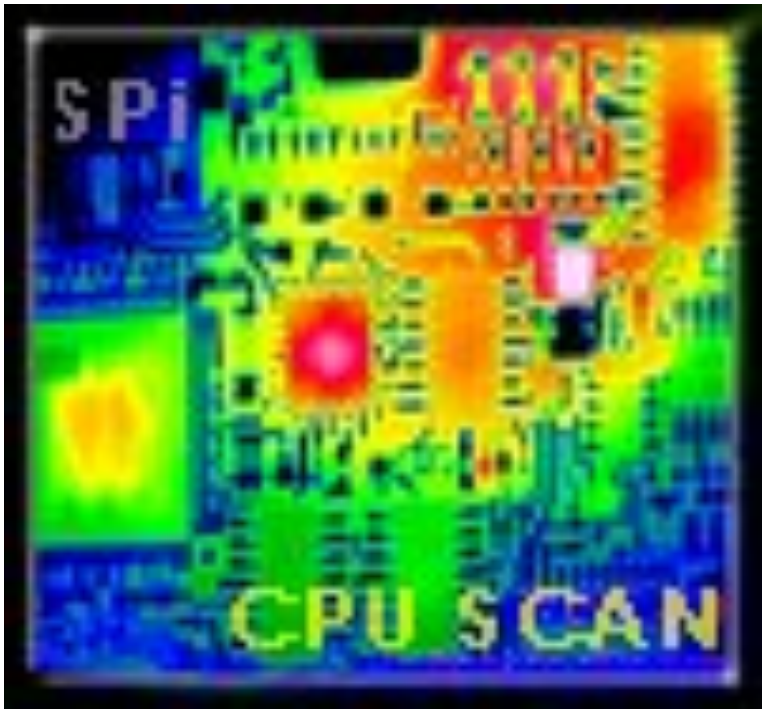

Applications

1) Arts and Sciences (astronomy, Oceanography, Meteorology, Geology, Vegetation and Soil, Animal Studies, Archeology, History and Arts

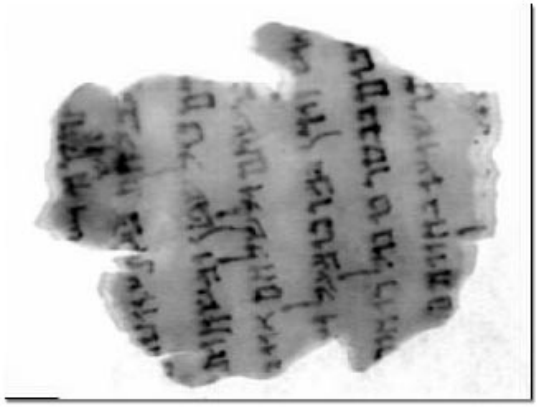

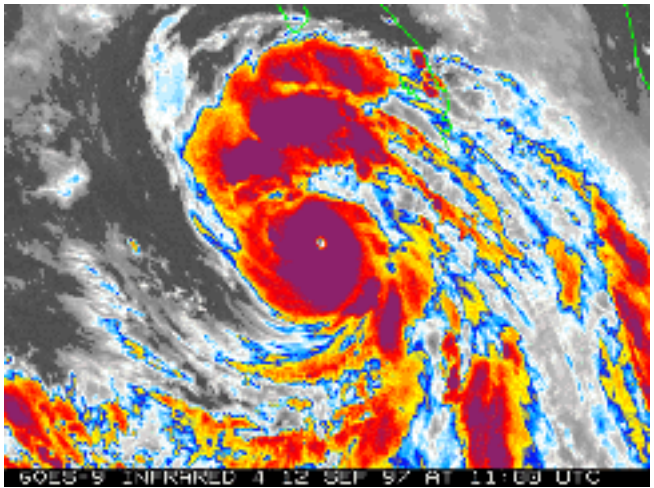

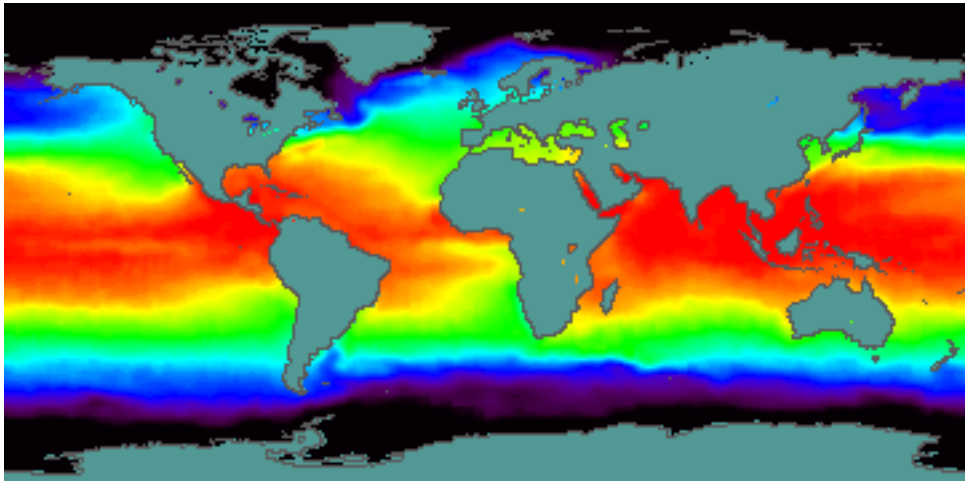

1800

Sir William Herschel Discovers Infrared Radiation.

William Herschel detects infrared light while measuring the temperatures in the colors of the spectrum created by passing sunlight through a prism. Herschel noticed that the temperature increased from the blue to the red part of the spectrum. He then measures the temperature in the region just past the red where there is no visible light, and to his surprise, this region registers the highest temperature of all. This experiment shows for the first time that there is light that we cannot see with our eyes. Infrared becomes the first form of invisible radiation to be discovered. Herschel's experiment also shows that the Sun is a source of infrared light.

1856

Infrared Detected From the Moon.

Infrared radiation is detected from the moon by Charles Piazzi Smyth from the peak of Guajara on Tenerife. He uses a thermocouple (a device which converts heat into electric current) to detect infrared light from the full moon. Piazzi also tests observations at different altitudes and shows that better observations are obtained at higher altitudes. This is the first indication that our atmosphere absorbs some of the infrared radiation from space.

1878

Infrared Bolometer Developed

The bolometer is developed by Samuel Pierpoint Langley. This instrument is an electrical detector of radiant heat which can detect a broader range of infrared wavelengths (far past the region of Herschel's discovery). Langley's bolometer is sensitive to differences in temperature of one hundred-thousandth of a degree Celsius (0.00001 C). The new bolometer is used to study the intensity of infrared radiation from the Sun.

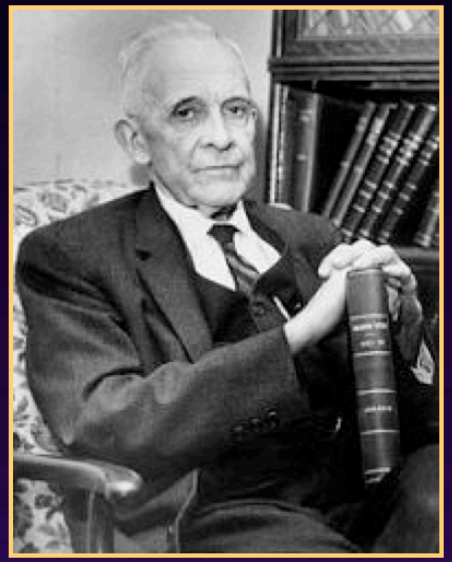

Early 1900s

Thermopile Detectors Developed
Infrared Detected From Jupiter, Saturn and Bright Stars

In 1915, William Coblentz develops thermopile detectors while working at the U.S. National Bureau of Standards. Thermopile detectors are basically several thermocouples joined together. He uses this new detector to measure the infrared radiation from 110 stars, as well as from planets, such as Jupiter and Saturn, and several nebulae. William Coblentz would become the founder of modern infrared spectroscopy.

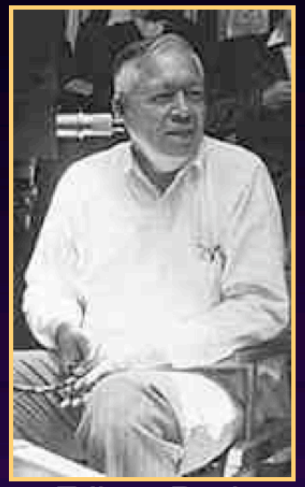

Edison Pettit

1920's

First Systematic Infrared Observations

The first systematic infrared observations of celestial objects are made by Seth B. Nicholson, Edison Pettit and other American astronomers. They use a vacuum thermocouple to measure the infrared radiation from the Moon, planets, sunspots, and stars. Their infrared studies allow them to make some of the first measurements of the diameters of giant stars.

Seth B. Nicholson

1948

Infrared Shows Moon Covered By Powder

Infrared studies of the Moon reveal that its surface is covered with a fine powder (more than 20 years before the Moon landings). This thick layer of powder is due to meteorite impacts over billions of years. It will later be found that this powder is two to ten meters thick in the lowlands and hundreds to thousands of meters thick in the lunar highlands.

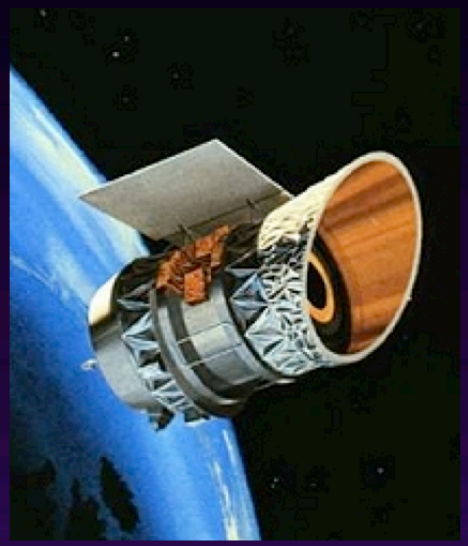

1983
First Infrared Space Observatory Launched

IRAS (Infrared Astronomical Satellite) is launched. For ten months IRAS scans more than 96 percent of the sky, providing the first high sensitivity all-sky map at wavelengths of 12, 25, 60 and 100 microns. IRAS doubles the number of cataloged astronomical sources by detecting about 500,000 infrared sources. IRAS discoveries include a disk of dust grains around the star Vega, six new comets, and very strong infrared emission from interacting galaxies, as well as wisps of warm dust called infrared cirrus which are found in almost every direction of space. IRAS also reveals for the first time the central core of our galaxy, the Milky Way.

1989
COBE Launched

NASA launches the Cosmic Background Explorer (COBE) in November 1989, to study both infrared and microwave characteristics of the cosmic background radiation (the remains of the extreme heat that was created by the Big Bang). Over the next four years, COBE maps the brightness of the entire sky at several infrared wavelengths and discovers that the cosmic background radiation is not entirely smooth, showing extremely small variations in temperature. These variations may have led to the formation of galaxies.

2003
The Spitzer Space Telescope Launches

The Spitzer Space Telescope was launched in August 2003. It is the last of NASA's "great observatories" in space. Spitzer is be much more sensitive than prior infrared missions and will study the universe at a wide range of infrared wavelengths. Spitzer will concentrate on the study of brown dwarfs, super planets, protoplanetary and planetary debris disks, ultraluminous galaxies, active galaxies, and deep surveys of the early universe.

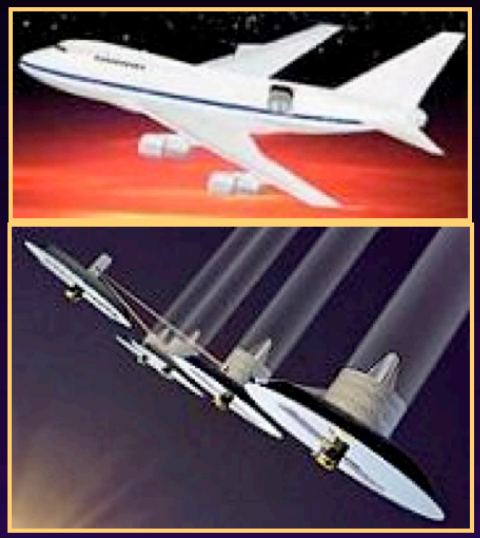

THE FUTURE

The future of infrared astronomy is very exciting. A new airborne observatory (SOFIA) will be the largest airborne telescope in the world. Ground-based observatories will benefit from rapidly improving technology. Several new infrared space missions are also being planned for launch within the next decade. These include Japan's IRIS mission, the European Space Agency's Herschel Space Observatory and Planck Surveyor, and NASA's James Webb Space Telescope and Terrestrial Planet Finder.

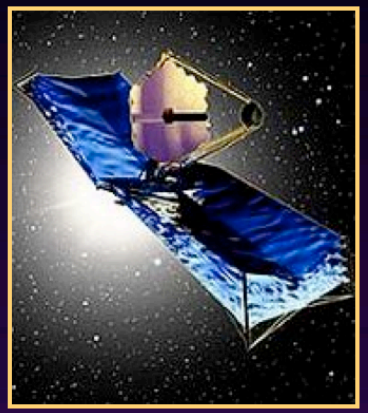

Atmospheric windows

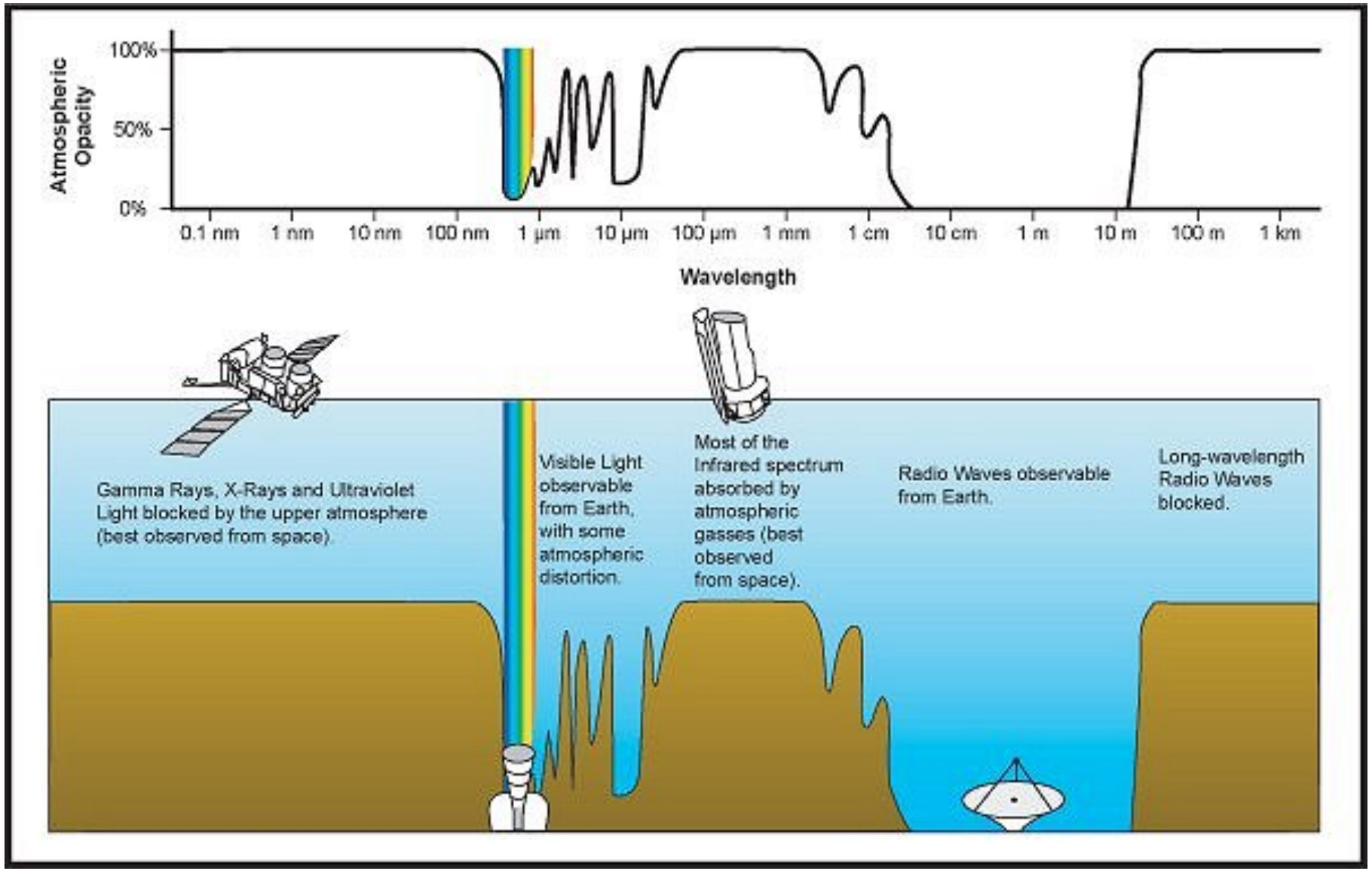

IR windows

Infrared Windows in the Atmosphere

Wavelength Range	Band	Sky Transparency	Sky Brightness
1.1 - 1.4 microns	J	high	low at night
1.5 - 1.8 microns	H	high	very low
2.0 - 2.4 microns	K	high	very low
3.0 - 4.0 microns	L	3.0 - 3.5 microns: fair 3.5 - 4.0 microns: high	low
4.6 - 5.0 microns	M	low	high
7.5 - 14.5 microns	N	8 - 9 microns and 10 -12 microns: fair others: low	very high
17 - 40 microns	17 - 25 microns: Q 28 - 40 microns: Z	very low	very high
330 - 370 microns		very low	low

Normal solar-type stars visible in the optical

- hydrogen burning
- layered, not fully convective like a BD
- $T_{eff} \sim 5000K$, maximum emission between 400nm - 700nm

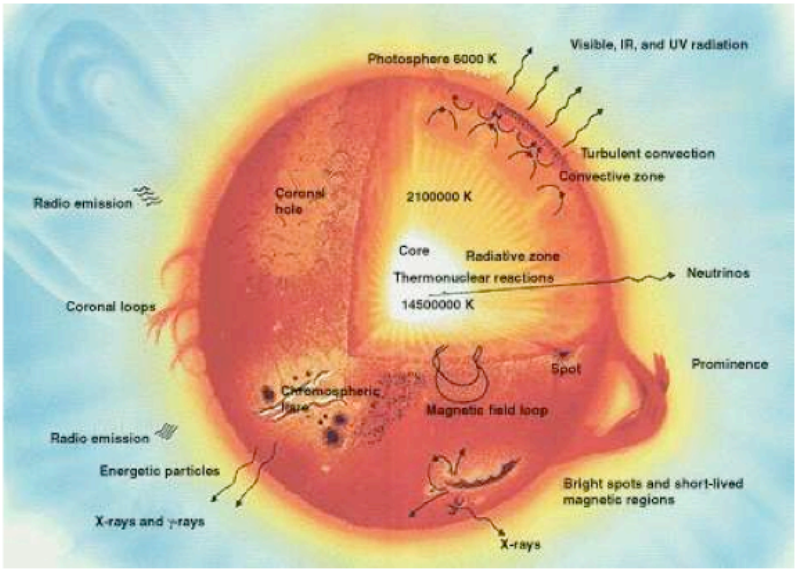

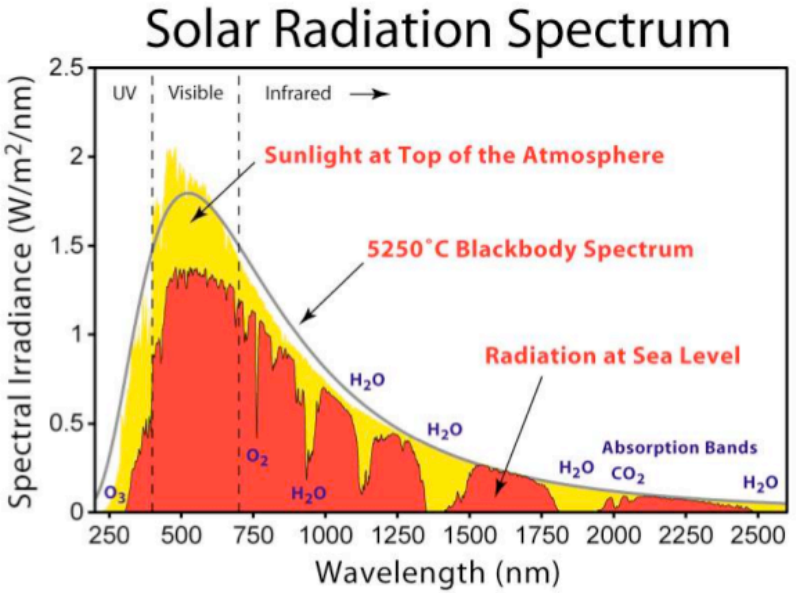

IR Observations

B68 molecular cloud (VLT *FORS* and *ISAAC*)

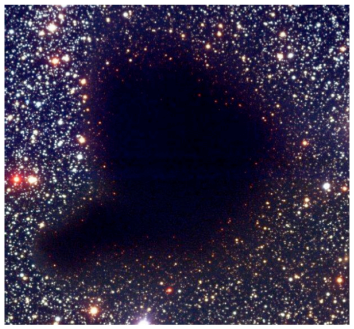

BVI

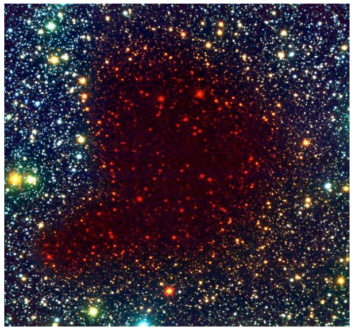

BIK

Near IR - dust becomes more transparent

As we enter the mid-infrared region of the spectrum, the cool stars begin to fade out

and cooler objects such as planets, comets and asteroids come into view.

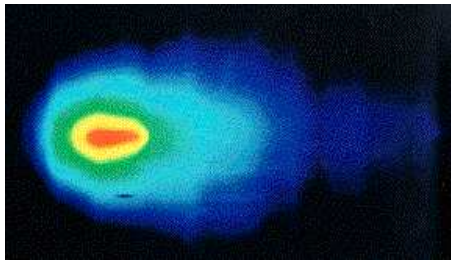

In the far-infrared, the stars have all vanished. Instead we now see very cold matter (140 Kelvin or less). Huge, cold clouds of gas and dust in our own galaxy, as well as in nearby galaxies, glow in far-infrared light.

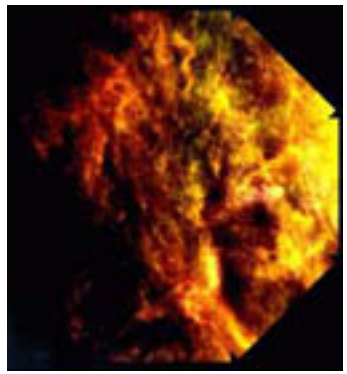

Near IR

- Commonly used filters: Z, J, H, K(s)
- Cover the stable parts of the transmissive windows
- Absorption caused by water vapour and CO_2

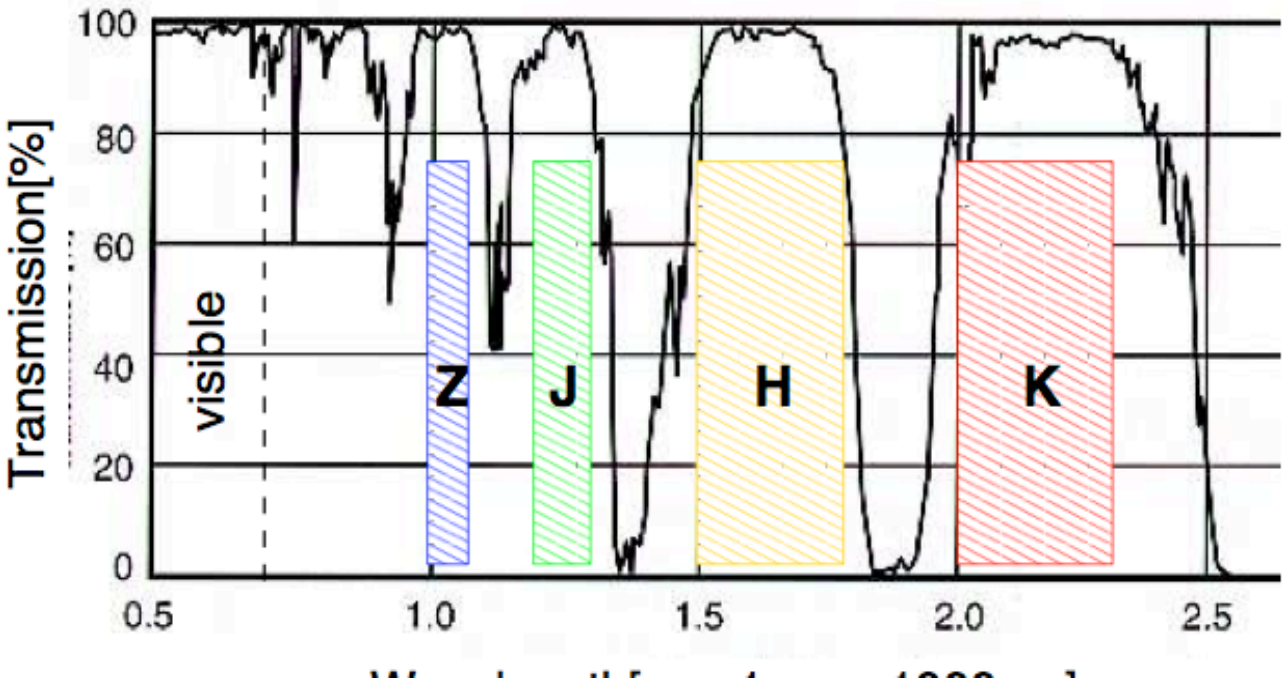

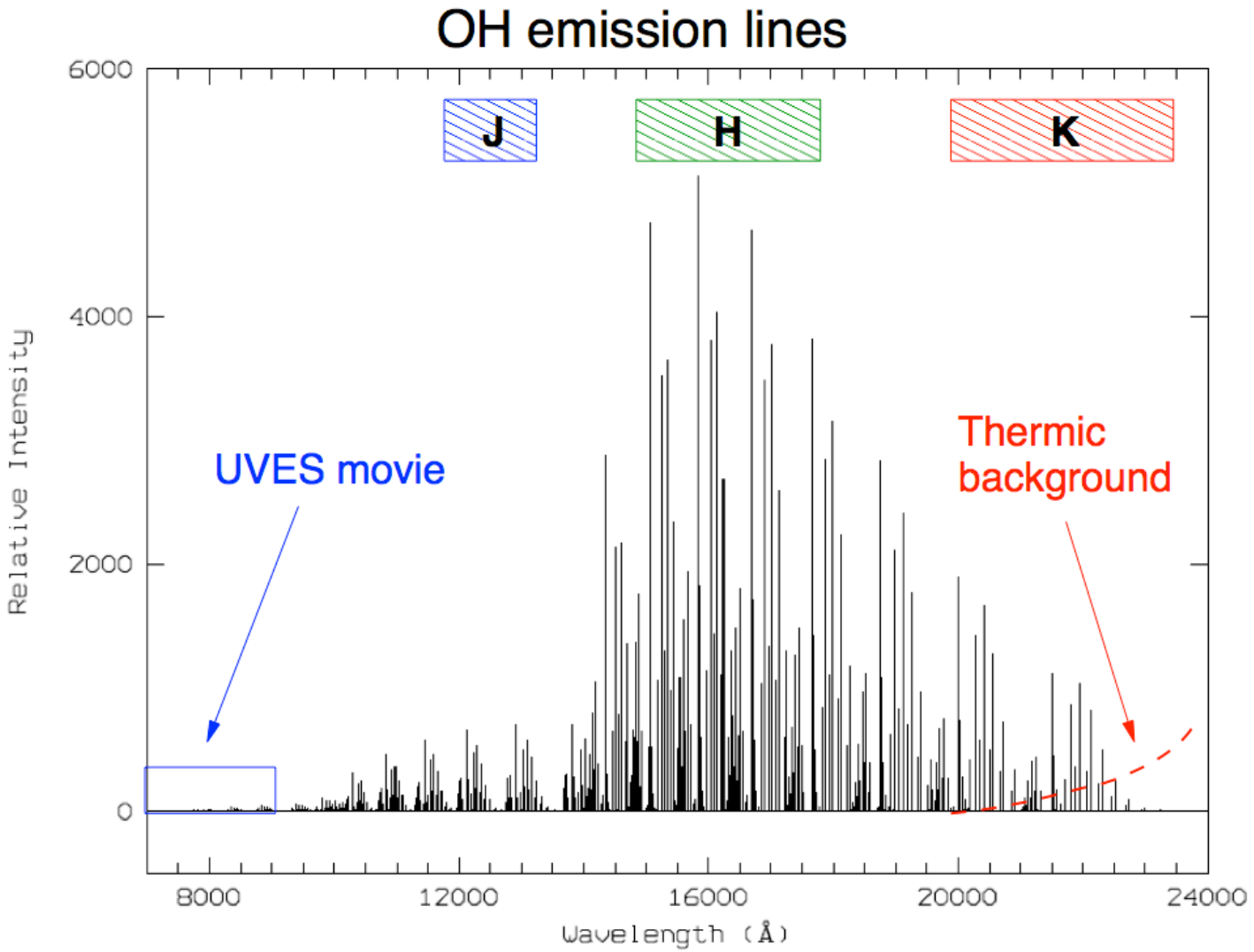

Night sky brightness:
[mag / arcsec^2]

$B = 22.7$
$V = 21.9$
$R = 21.0$
$I = 20.0$
$J = 16.0$
$H = 14.5$
$K = 13.5$

Short exposure times:
30, 20, 10s in J, H, K

Too many NIR systems

ESO SAAO NICMOS CIT

UKIRT 2MASS VISTA

Carpenter et al. 2001 transformations between Different systems.

Seeing unvisible

B68 molecular cloud (VLT *FORS* and *ISAAC*)

BVI

BIK

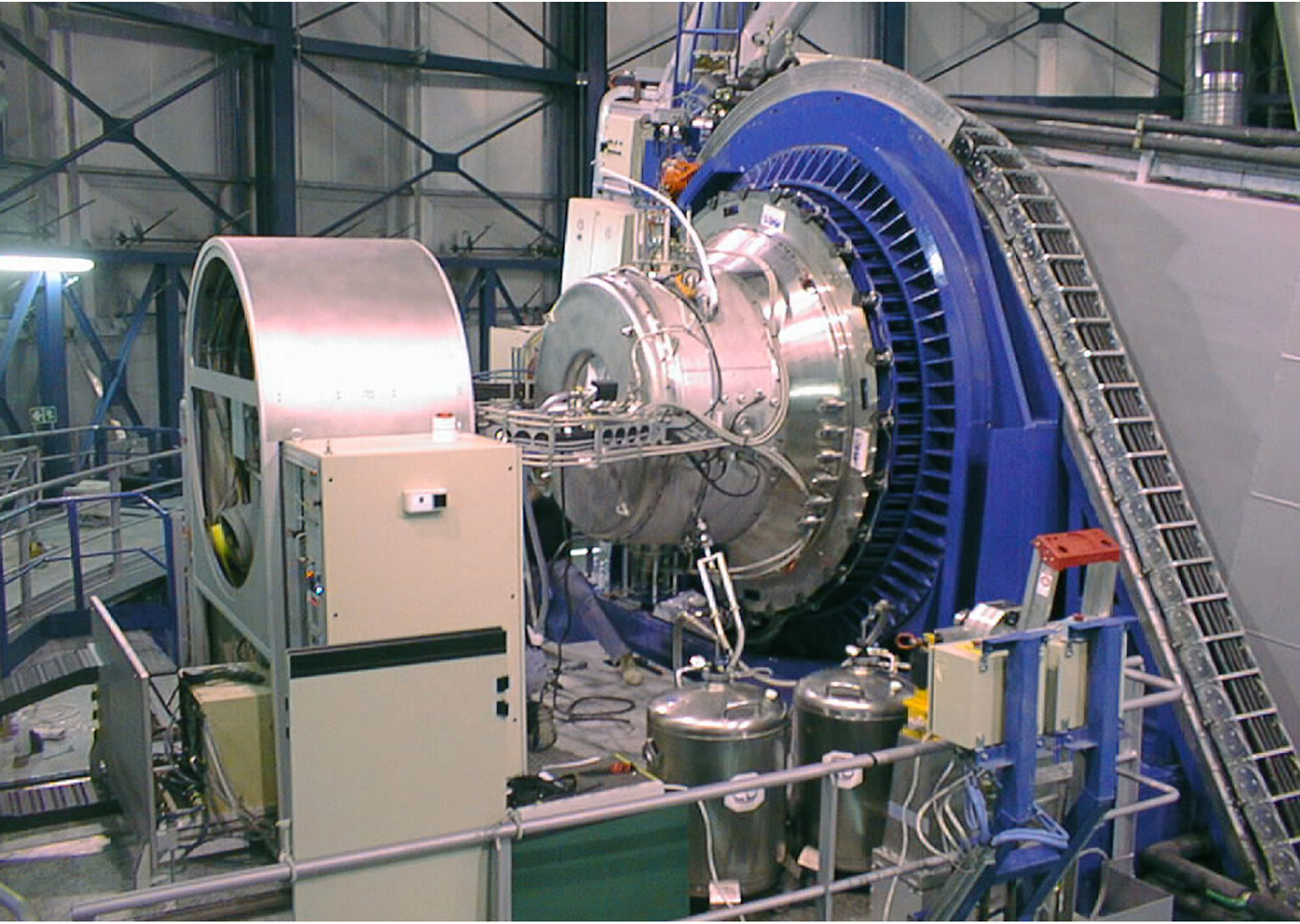

- Usually 1k×1k or 2k×2k HgCdTe detectors
- About 90% quantum efficiency from Z to K
- Operating temperature: 65-75 K
- Liquid nitrogen and helium cooling
- Very sensitive

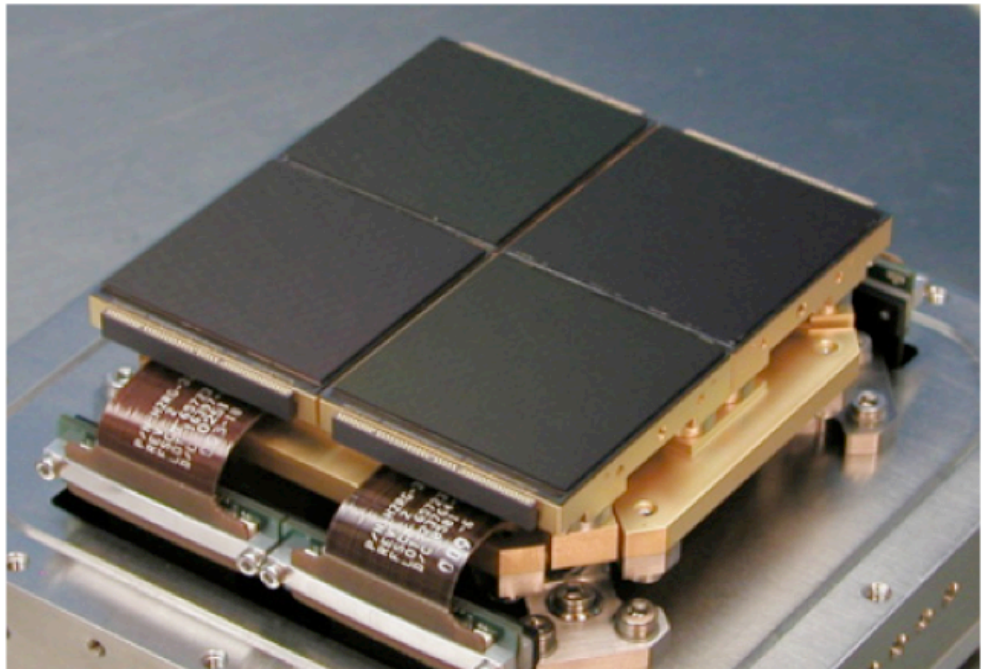

Left: HAWK-I detector mosaic at the VLT

4 $2k \times 2k$ detectors

Pixel scale: 0.106 arcsec

Field of view: 7.5 arcmin

Observations – simple jittering

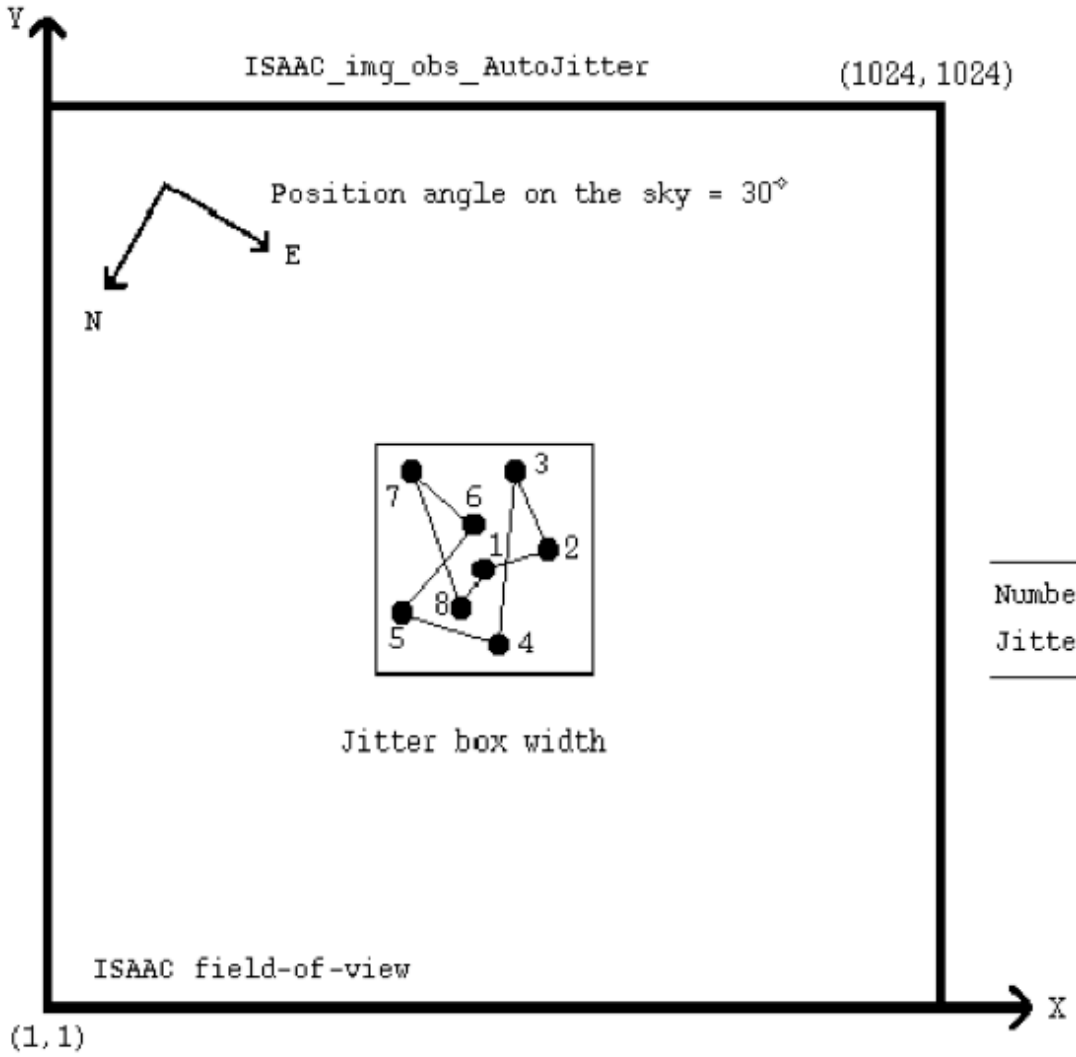

Template Parameters	
Number of exposures	8
Jitter box width	30"

Table 16: Overheads – Example 1 – SW: Imaging with the Hawaii

Template parameters	
Acquisition Template	`ISAACSW_img_acq_Preset`
Observation Template	`ISAACSW_img_obs_AutoJitter`
`DIT`	10 (seconds)
`NDIT`	10
`Number of Exposures`	36
Execution time (minutes)	
Preset	6.0
Instrument setup	0.5
int time + detector overhead	$(0.167 + 0.07) \times 10$ (`NDIT`) $\times$ 36
Telescope offsets	0.25×36
Total	101 minutes for 60 minutes of integration

ISAACSW_img_obs_FixedSkyOffset

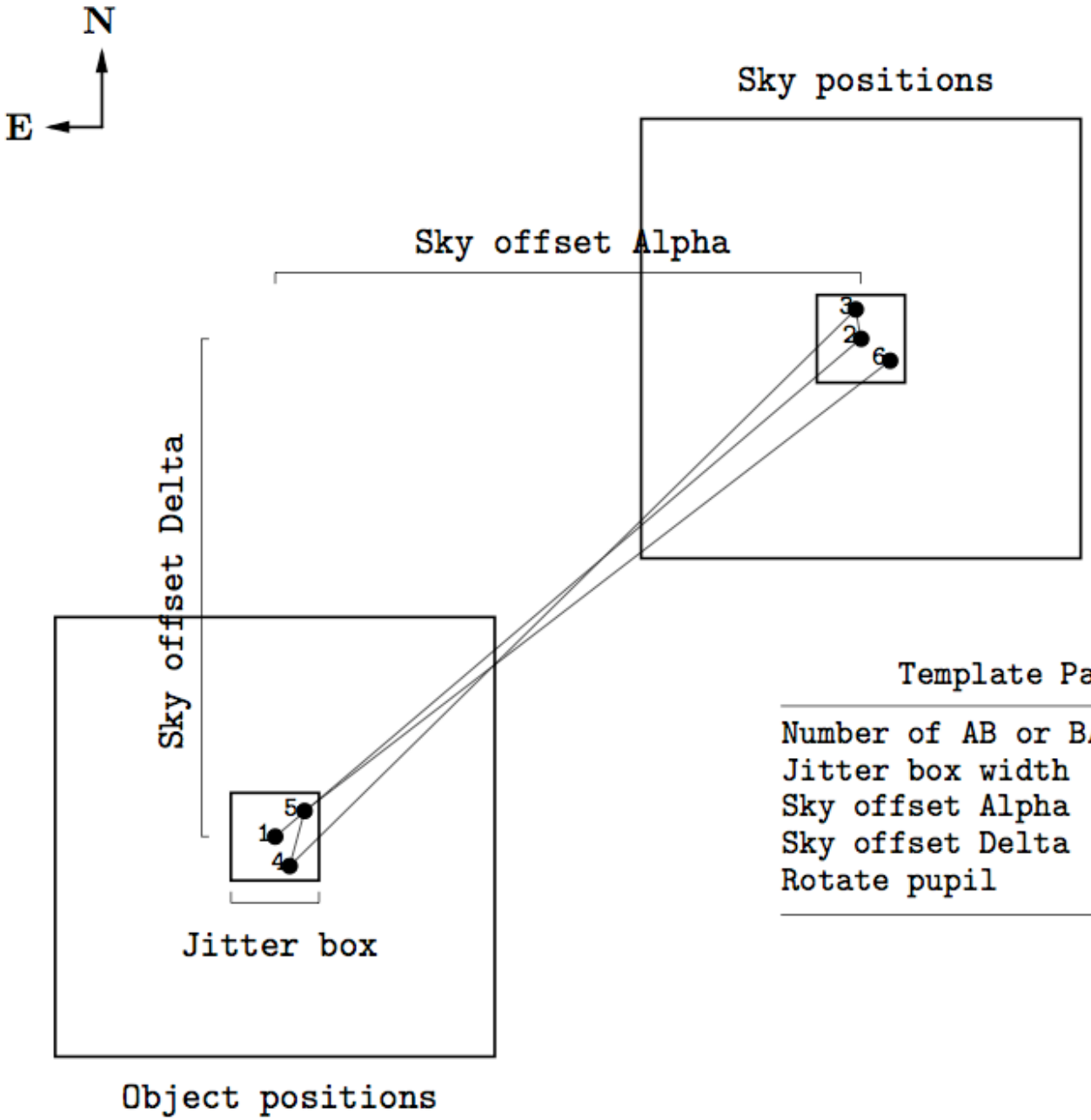

Template Parameters	
Number of AB or BA cycles	3
Jitter box width	30″
Sky offset Alpha	-200″
Sky offset Delta	170″
Rotate pupil	F

Observations

1) Standard star
2) Faint star low density field (LF)
3) Small globular cluster
4) Cepheids in a galaxy at 1-10 Mpc
5) Galactic Bulge

Reductions

1) Xdimsum (IRAF)

2) Eclipse (ESO) + other packages

3) Other software

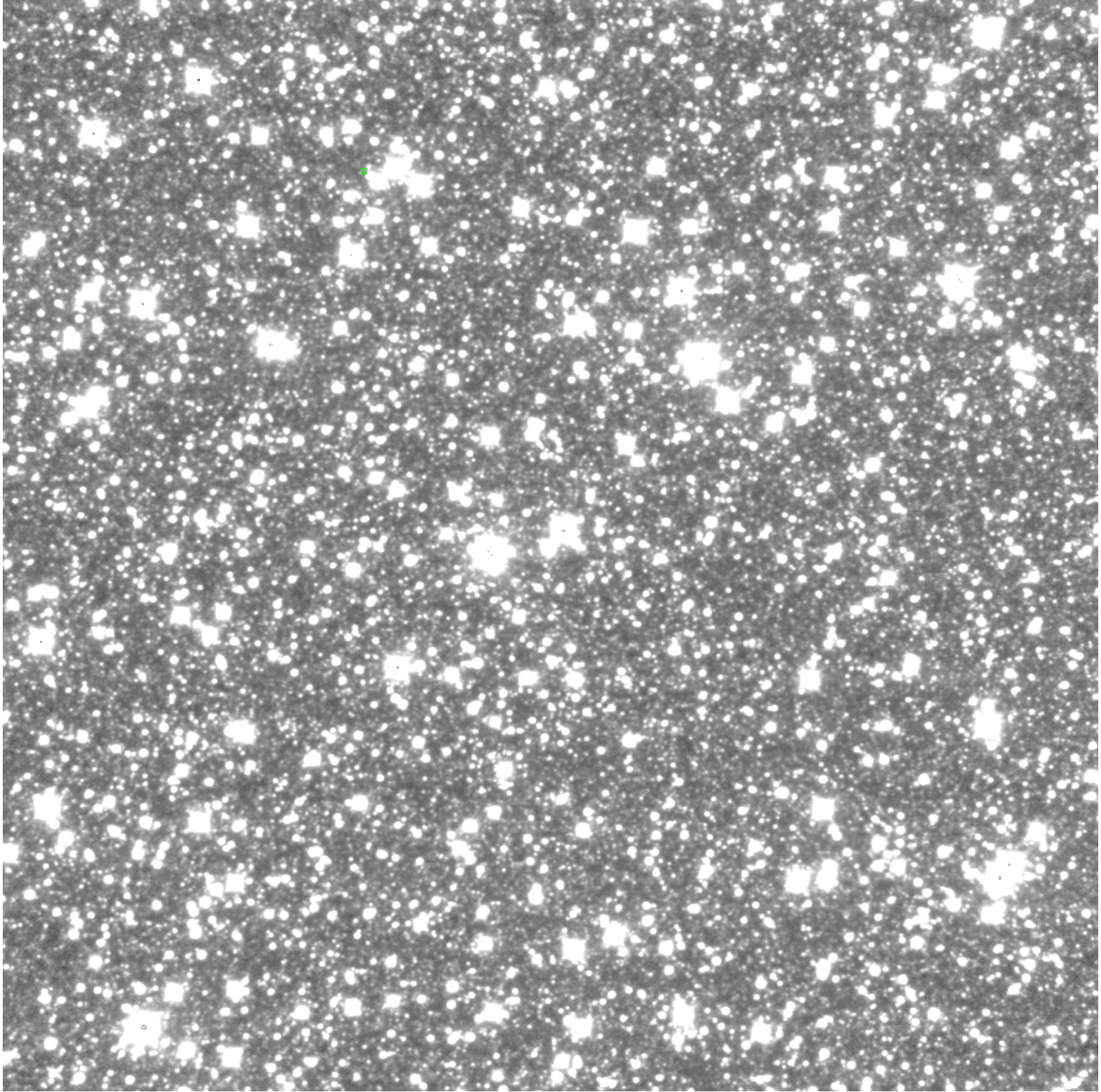

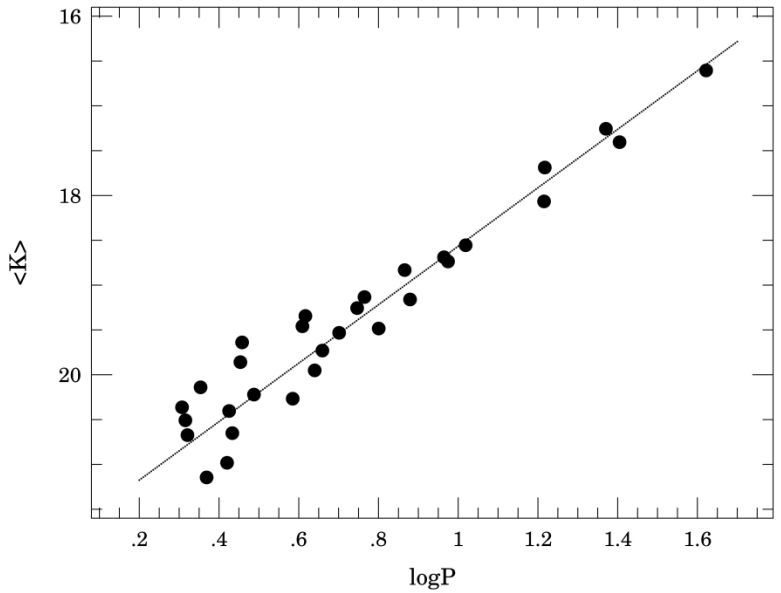
<K>
16
18
20
.2
.4
.6
.8
1
1.2
1.4
1.6
logP

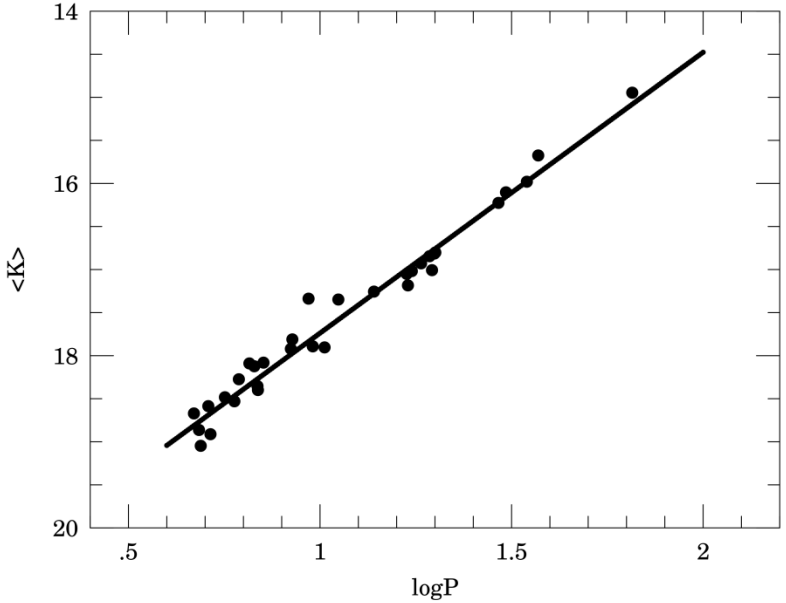
<K>
14
16
18
20
.5
1
1.5
2
logP

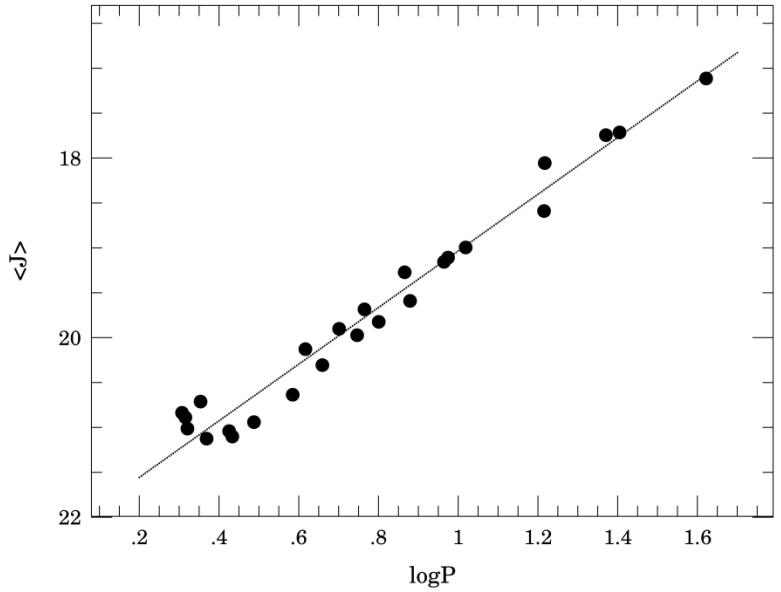
<J>
18
20
22
.2
.4
.6
.8
1
1.2
1.4
1.6
logP

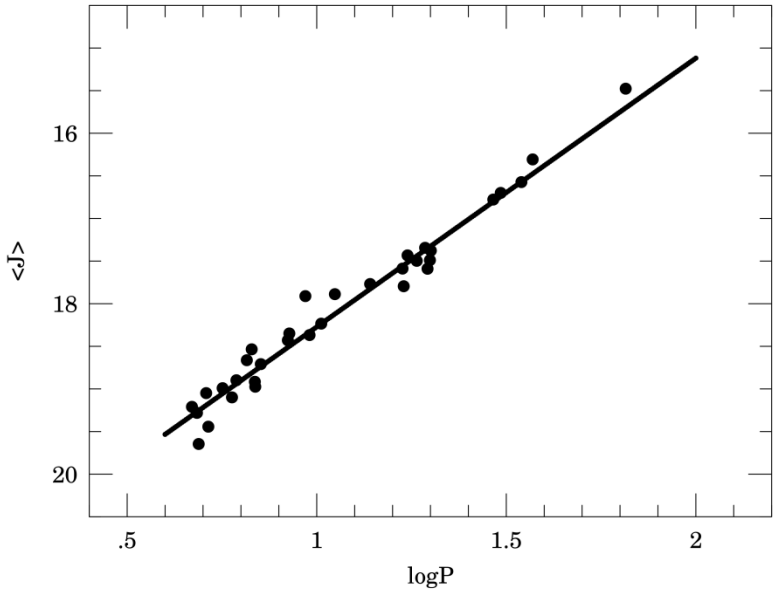
<J>
16
18
20
.5
1
1.5
2
logP

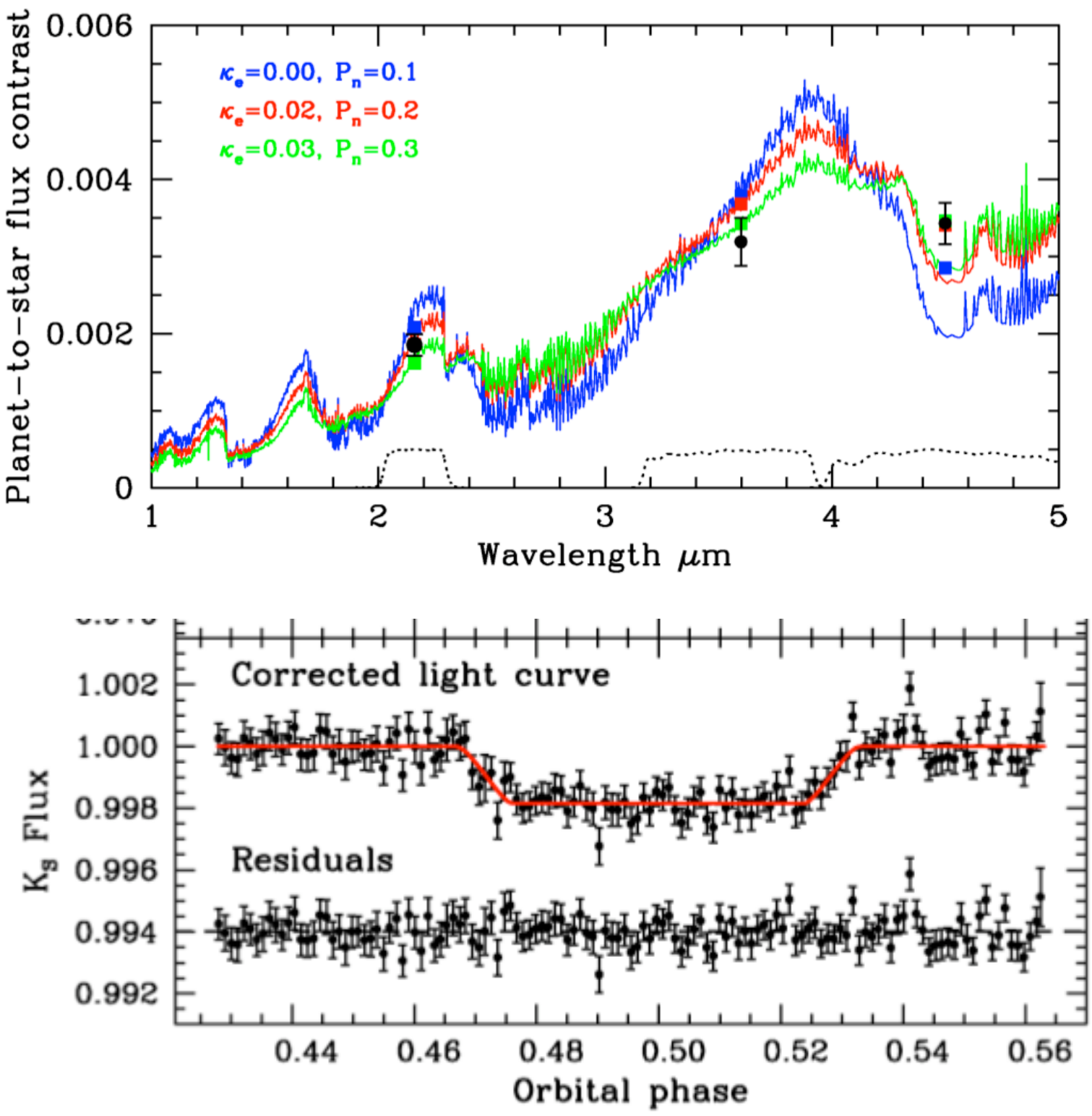
Planet−to−star flux contrast
0.006
0.004
0.002
0
1
2
3
4
5
Wavelength μm
κe=0.00, Pn=0.1
κe=0.02, Pn=0.2
κe=0.03, Pn=0.3
Corrected light curve
Residuals
Ks Flux
1.002
1.000
0.998
0.996
0.994
0.992
0.44
0.46
0.48
0.50
0.52
0.54
0.56
Orbital phase

AGN at z ~ 2 in NIR !

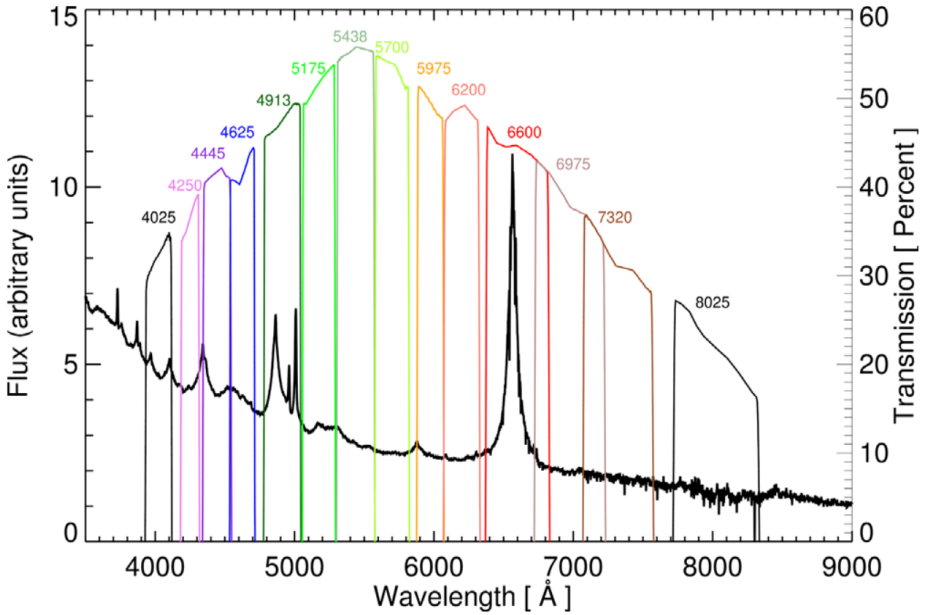

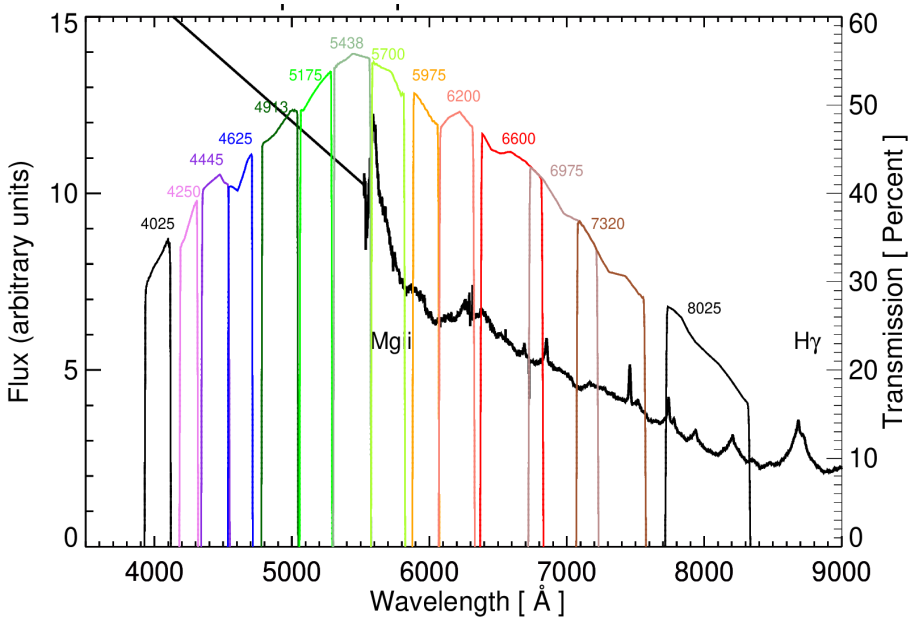

Adaptive optics

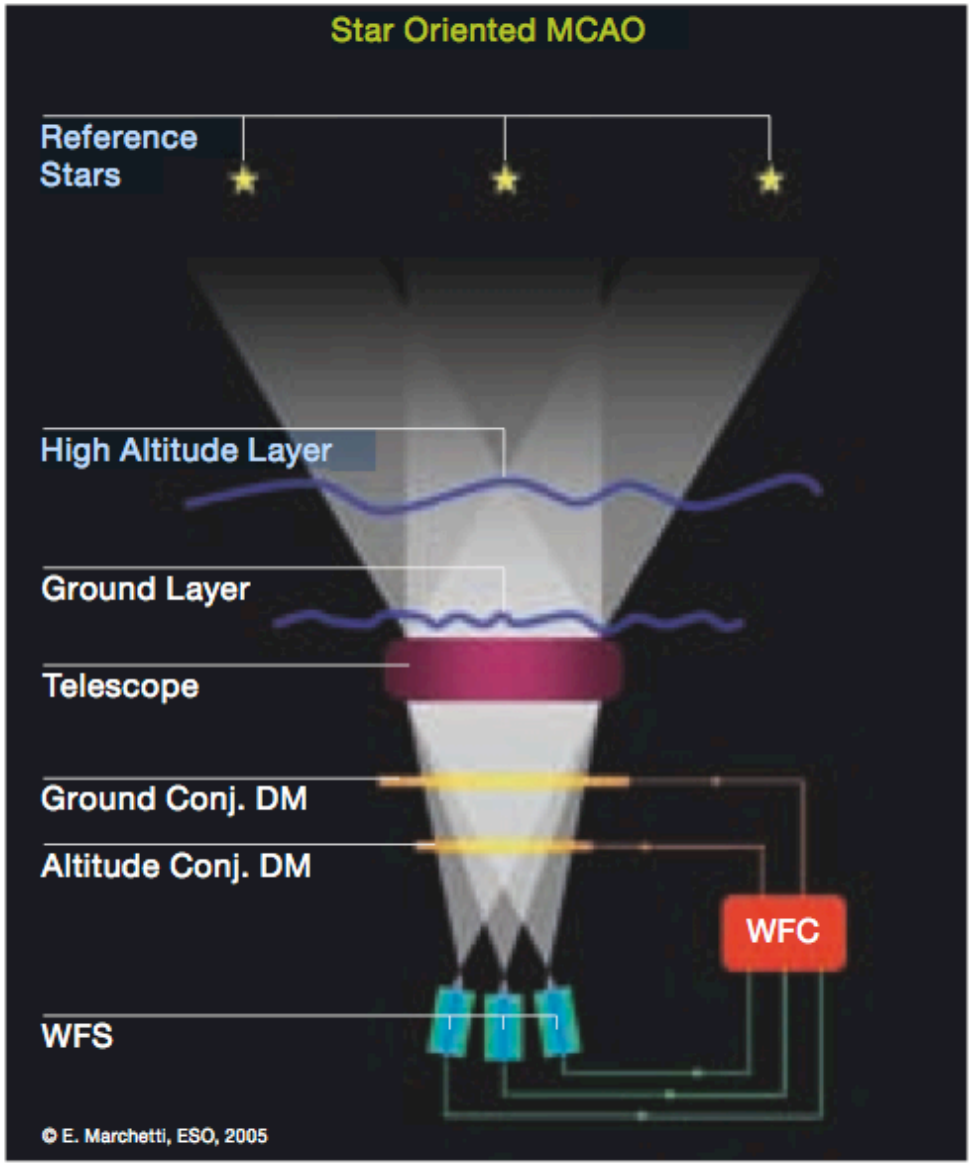

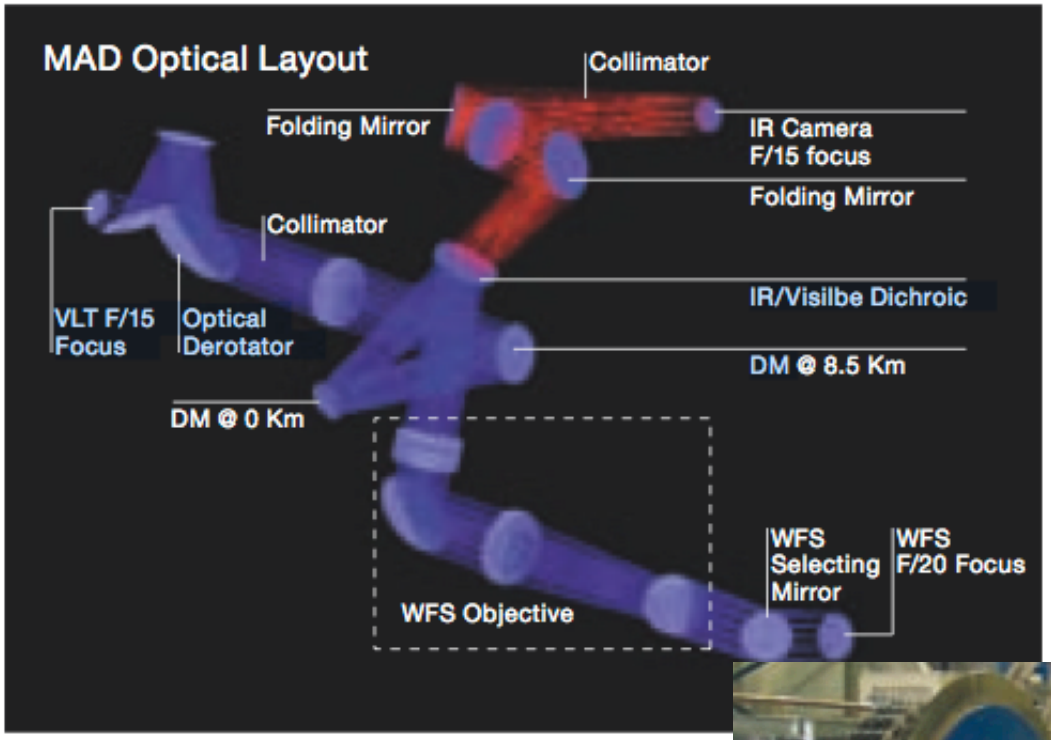
MAD Optical Layout
Collimator
Folding Mirror
IR Camera
F/15 focus
Folding Mirror
Collimator
VLT F/15
Focus
Optical
Derotator
IR/Visilbe Dichroic
DM @ 8.5 Km
DM @ 0 Km
WFS
Selecting
Mirror
WFS
F/20 Focus
WFS Objective

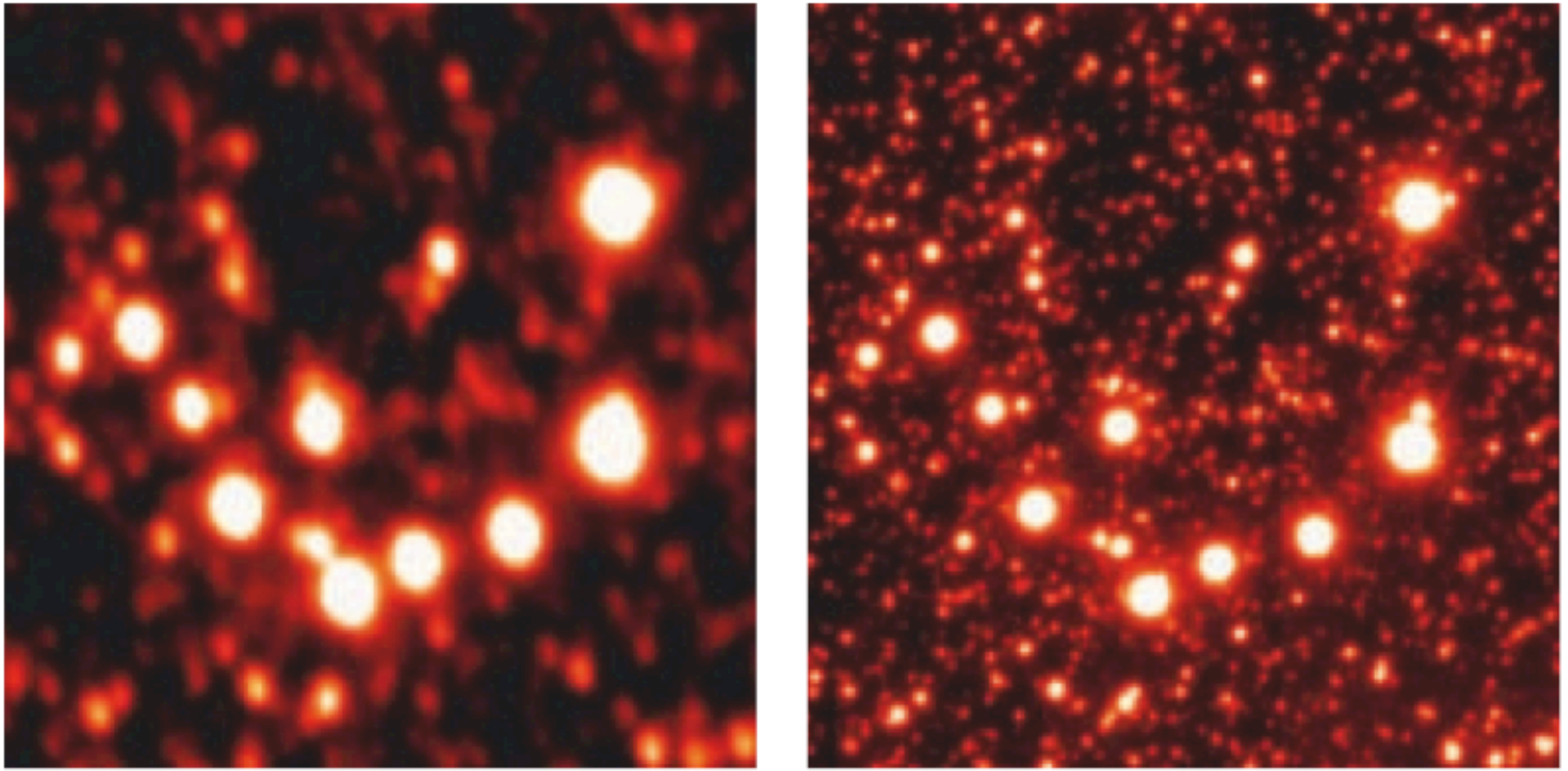

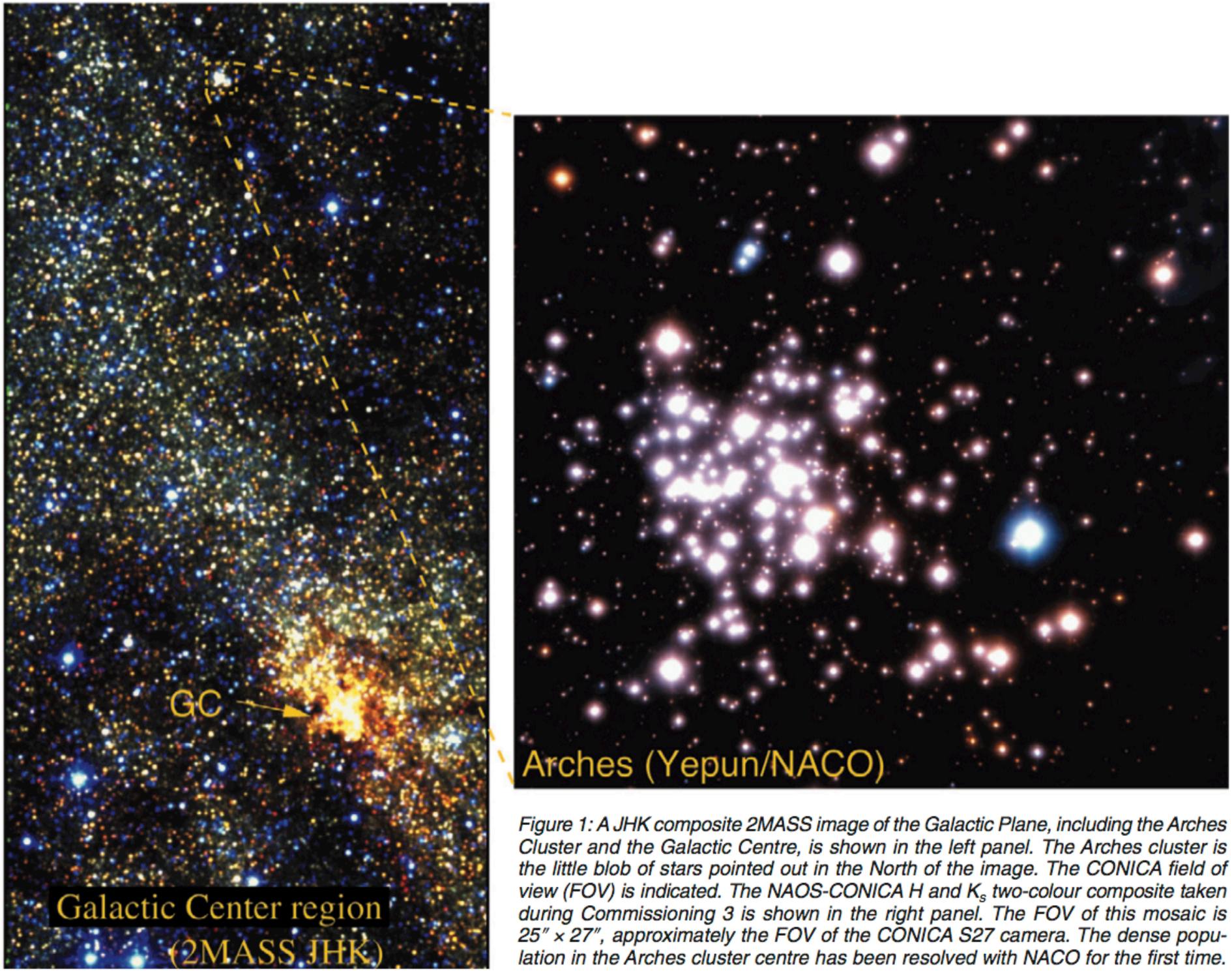

Figure 1: A JHK composite 2MASS image of the Galactic Plane, including the Arches Cluster and the Galactic Centre, is shown in the left panel. The Arches cluster is the little blob of stars pointed out in the North of the image. The CONICA field of view (FOV) is indicated. The NAOS-CONICA H and K_s two-colour composite taken during Commissioning 3 is shown in the right panel. The FOV of this mosaic is 25″ × 27″, approximately the FOV of the CONICA S27 camera. The dense population in the Arches cluster centre has been resolved with NACO for the first time.

Distance scale

- population effects (e.g. Cepheids)
- extinction (internal extinction, reddening law)
- SBCR for late type stars is optimal for V-K color ⋯
- A must to use AGNs
- Infrared interferometry

Spectroscopy

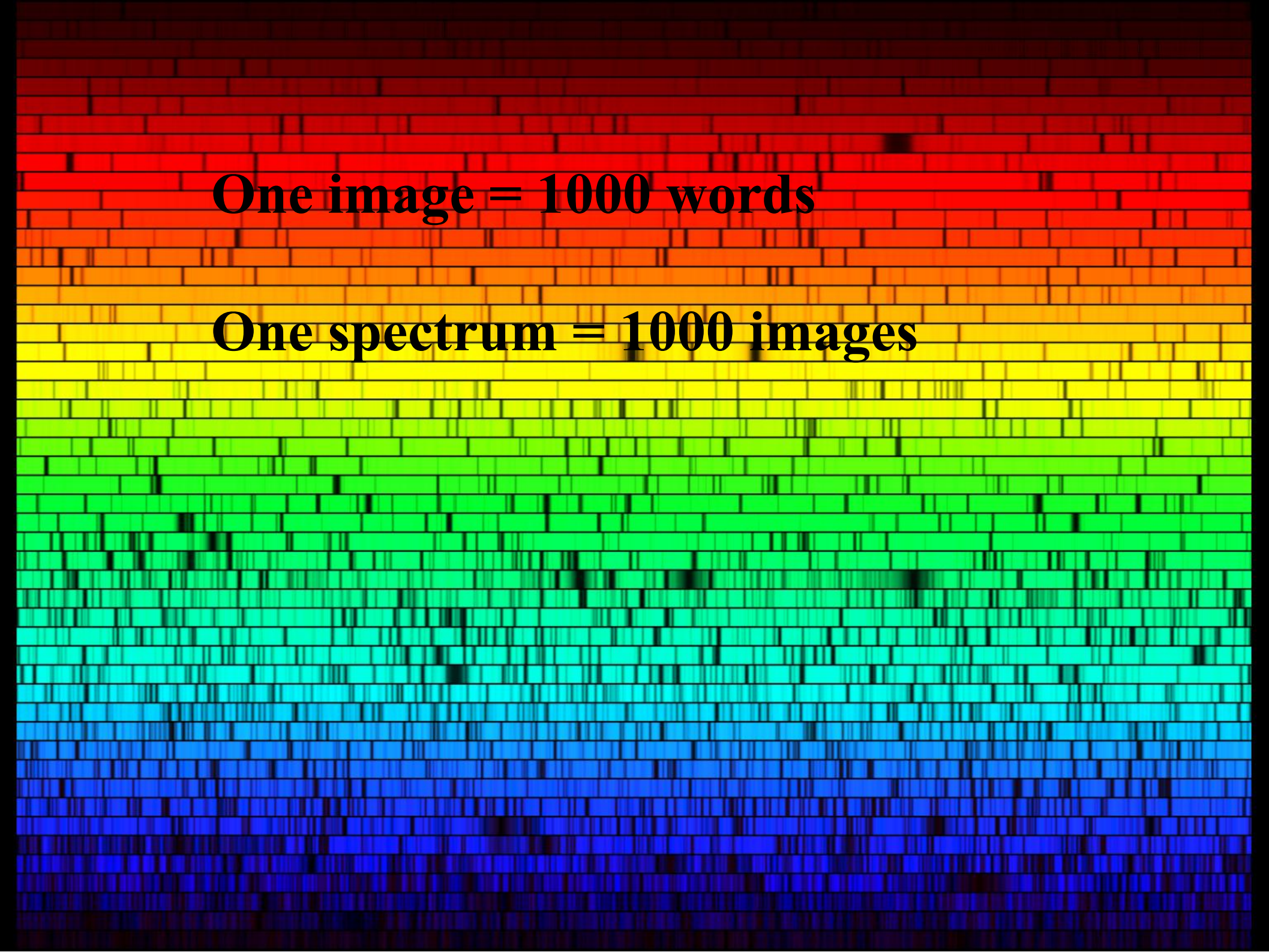
One image = 1000 words
One spectrum = 1000 images

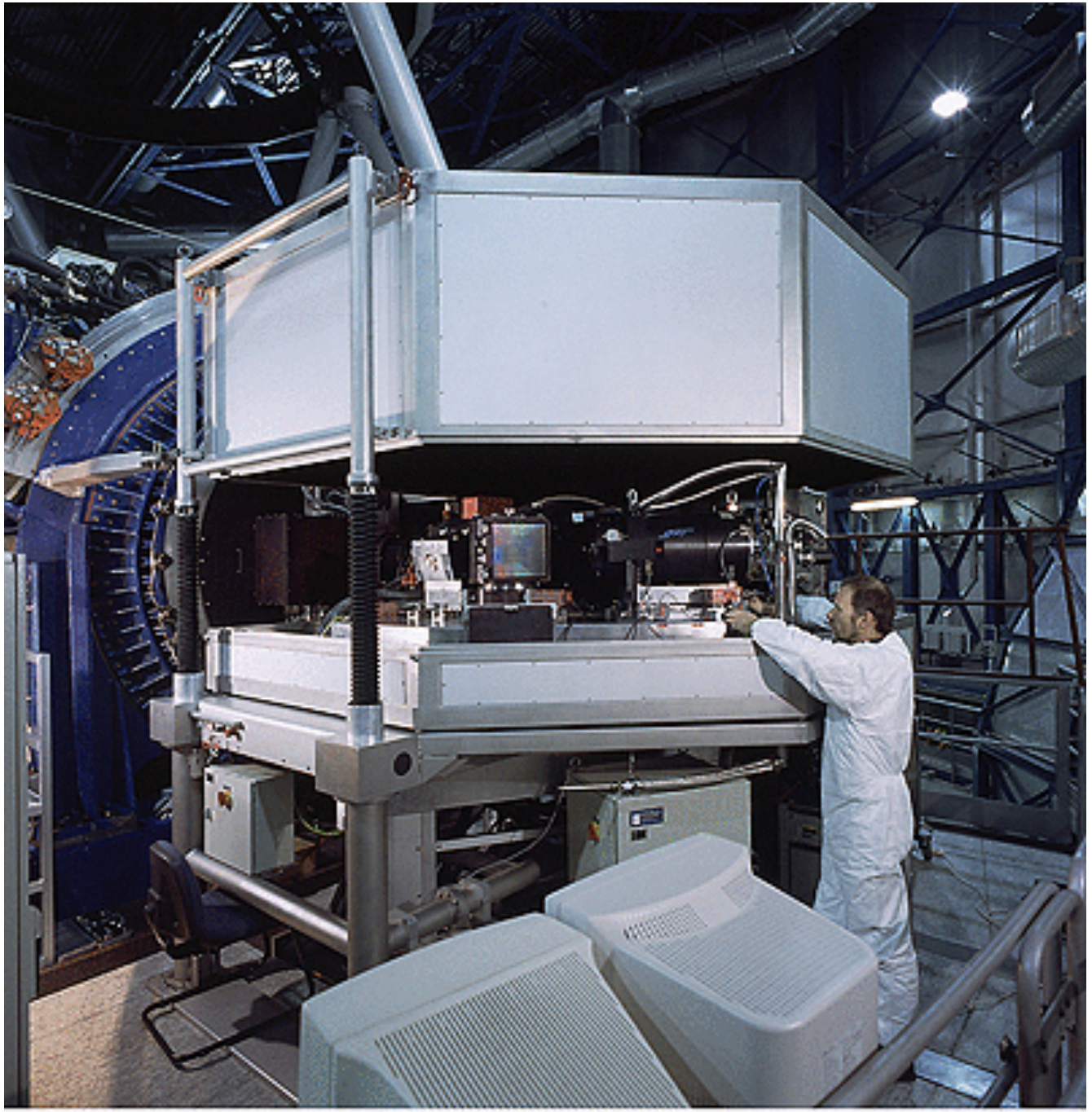

UVES at Kueyen

ESO PR Photo 43c/99 (8 December 1999)

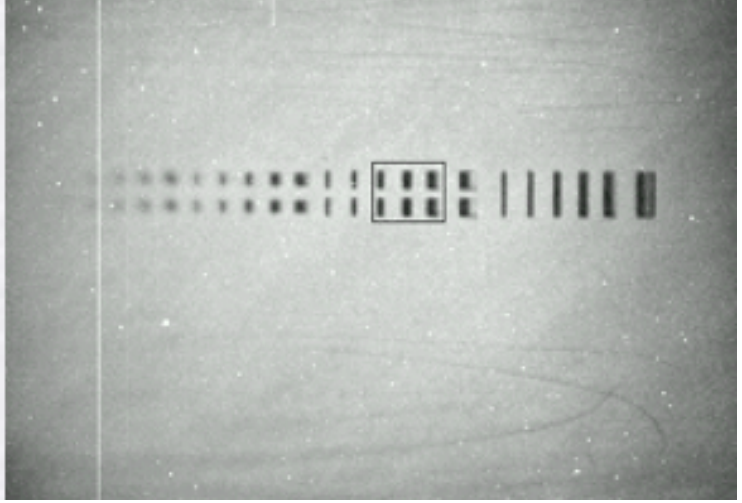

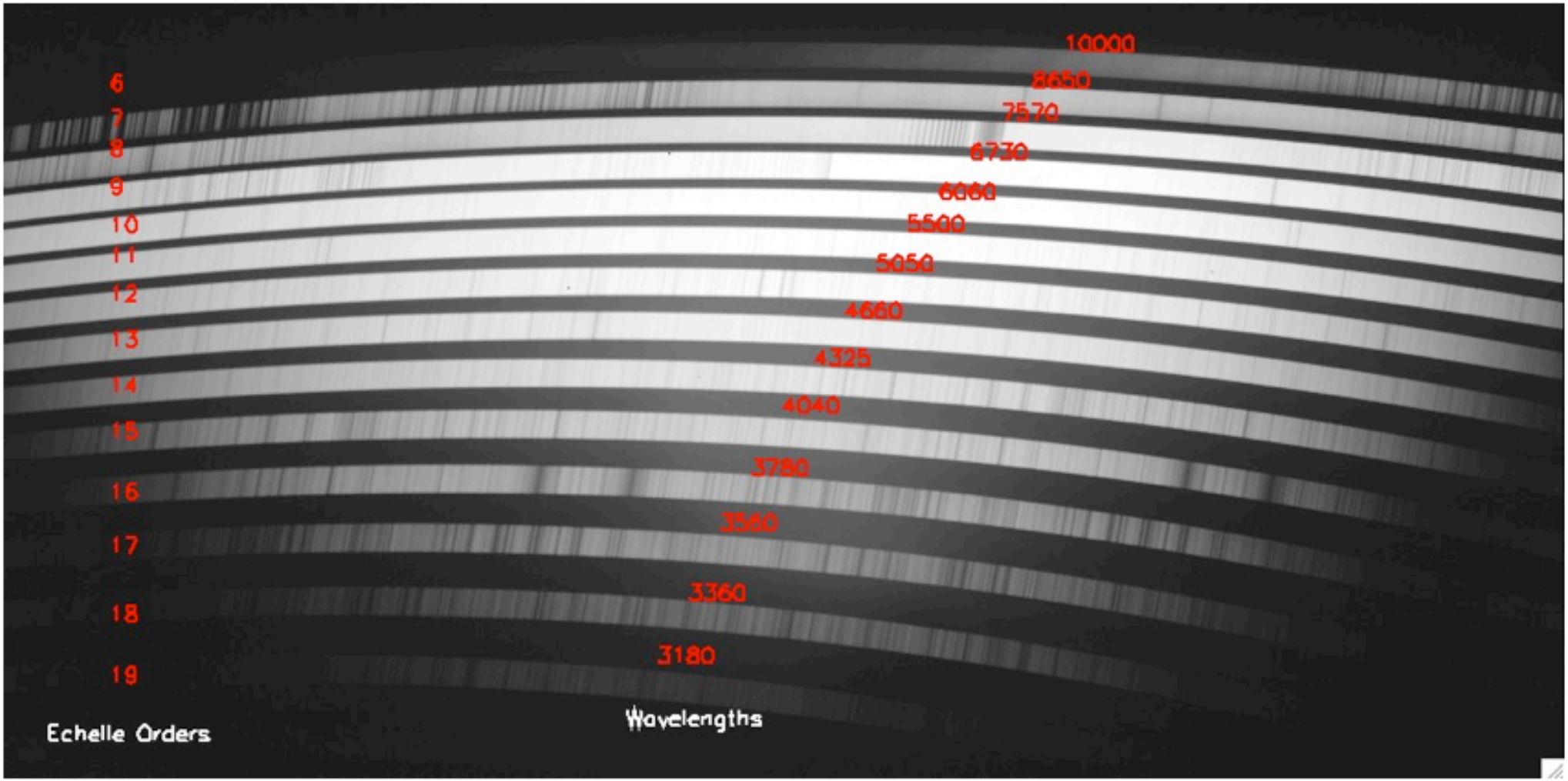
10000
8650
7570
6730
6060
5500
5050
4660
4325
4040
3780
3560
3360
3180
6
7
8
9
10
11
12
13
14
15
16
17
18
19
Wavelengths
Echelle Orders

Calibrations

Bias

Flat Field (difficult)

Order definition

Internal lamps (wavelength calibration)

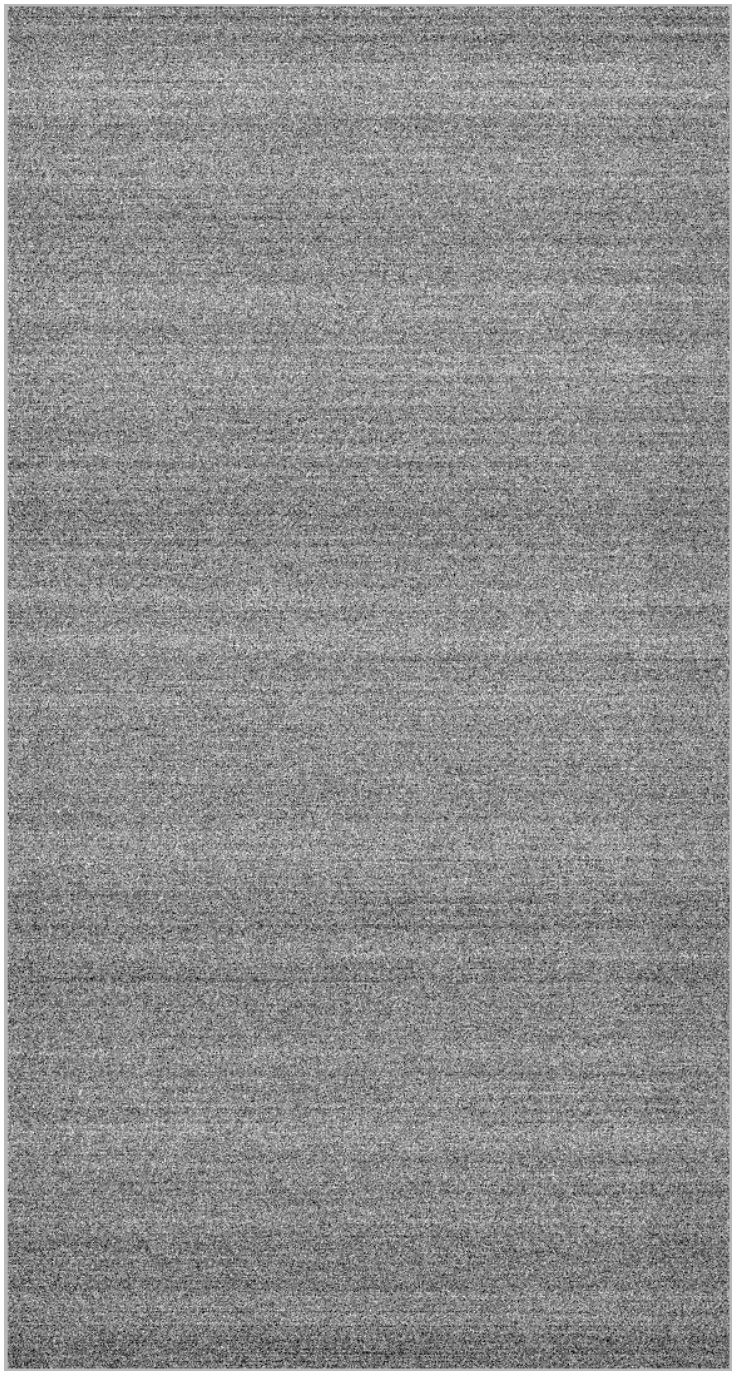

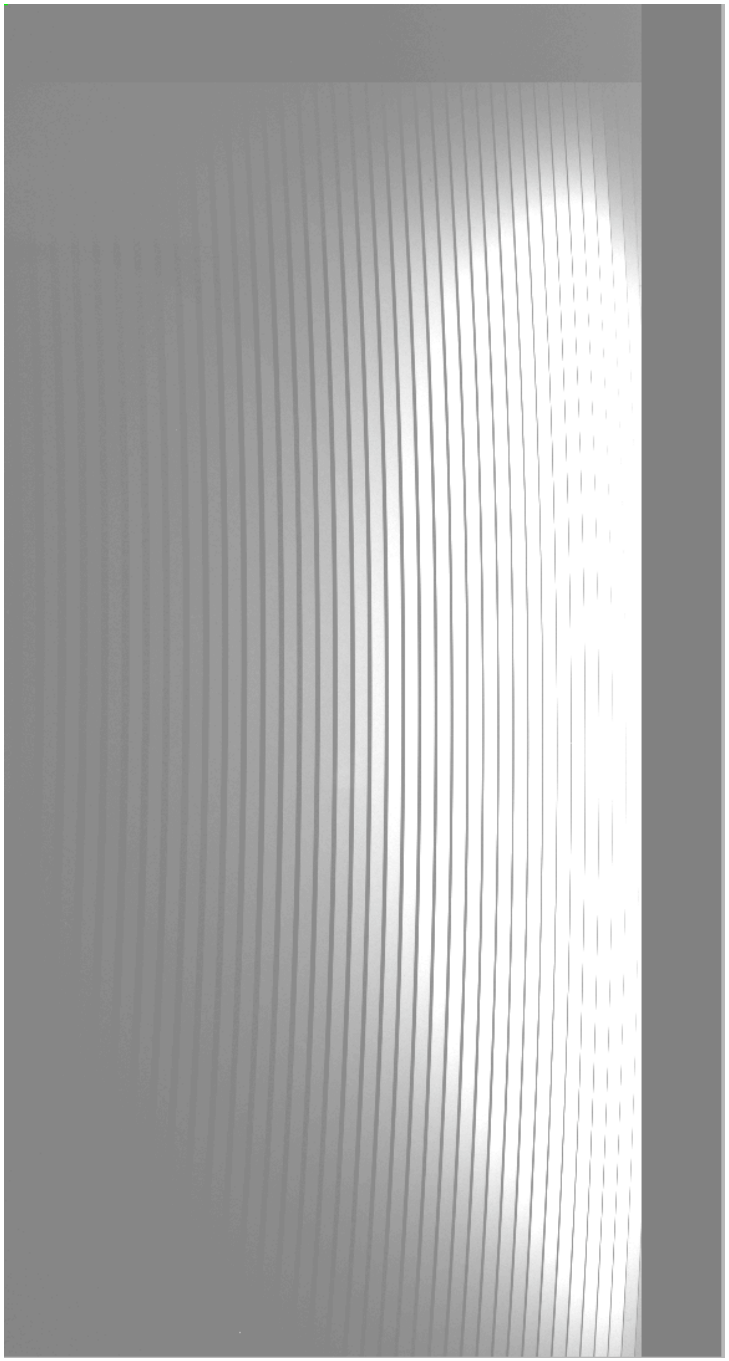

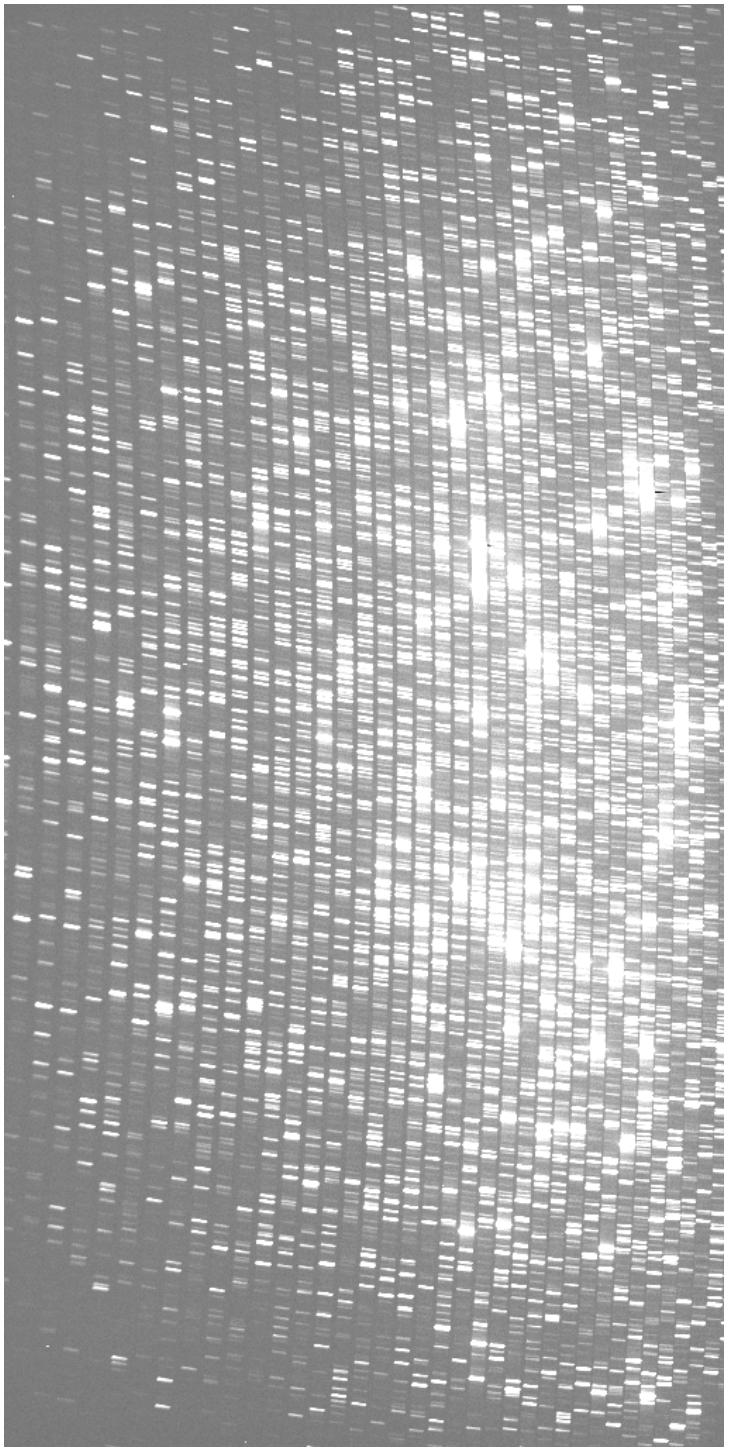

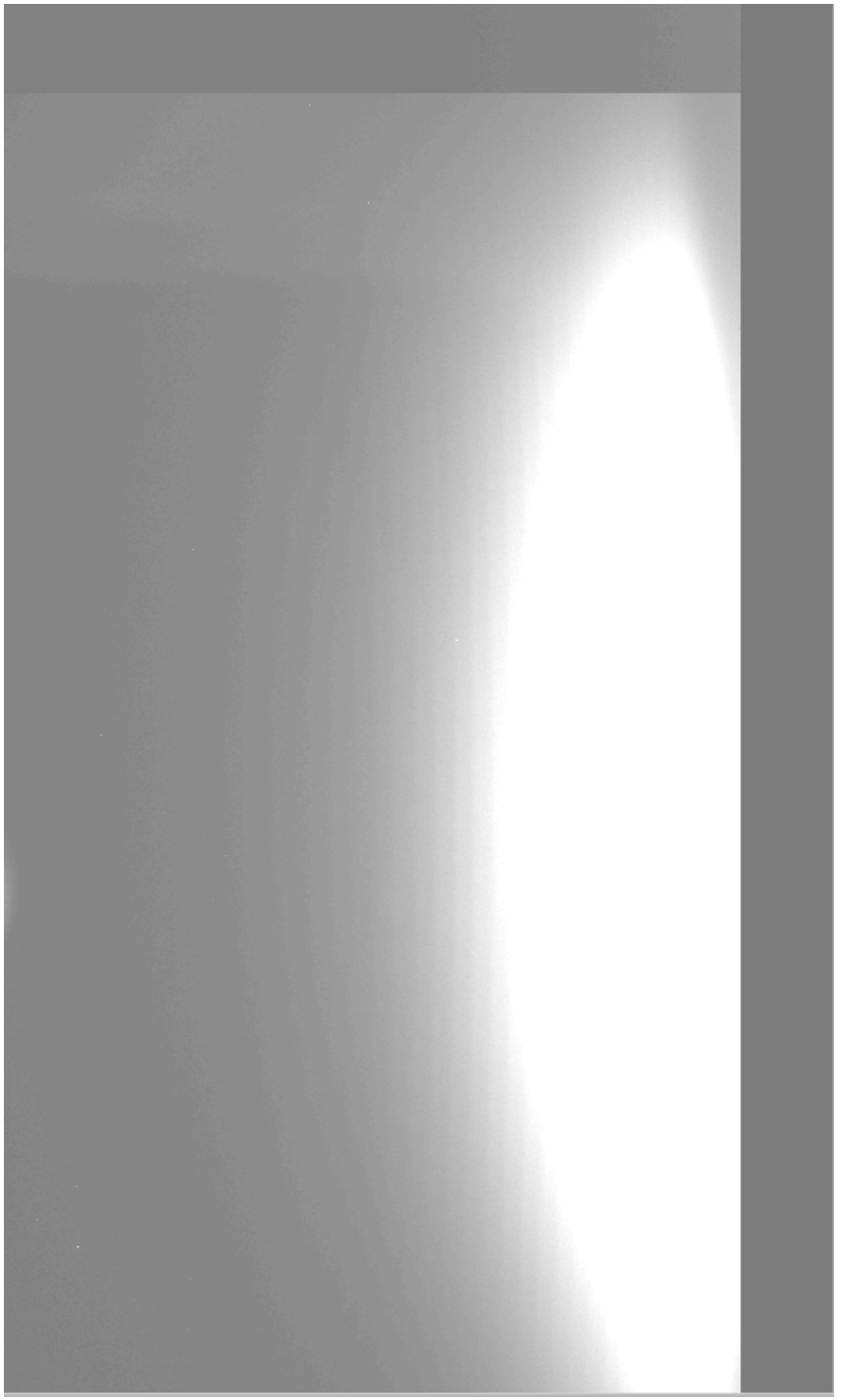

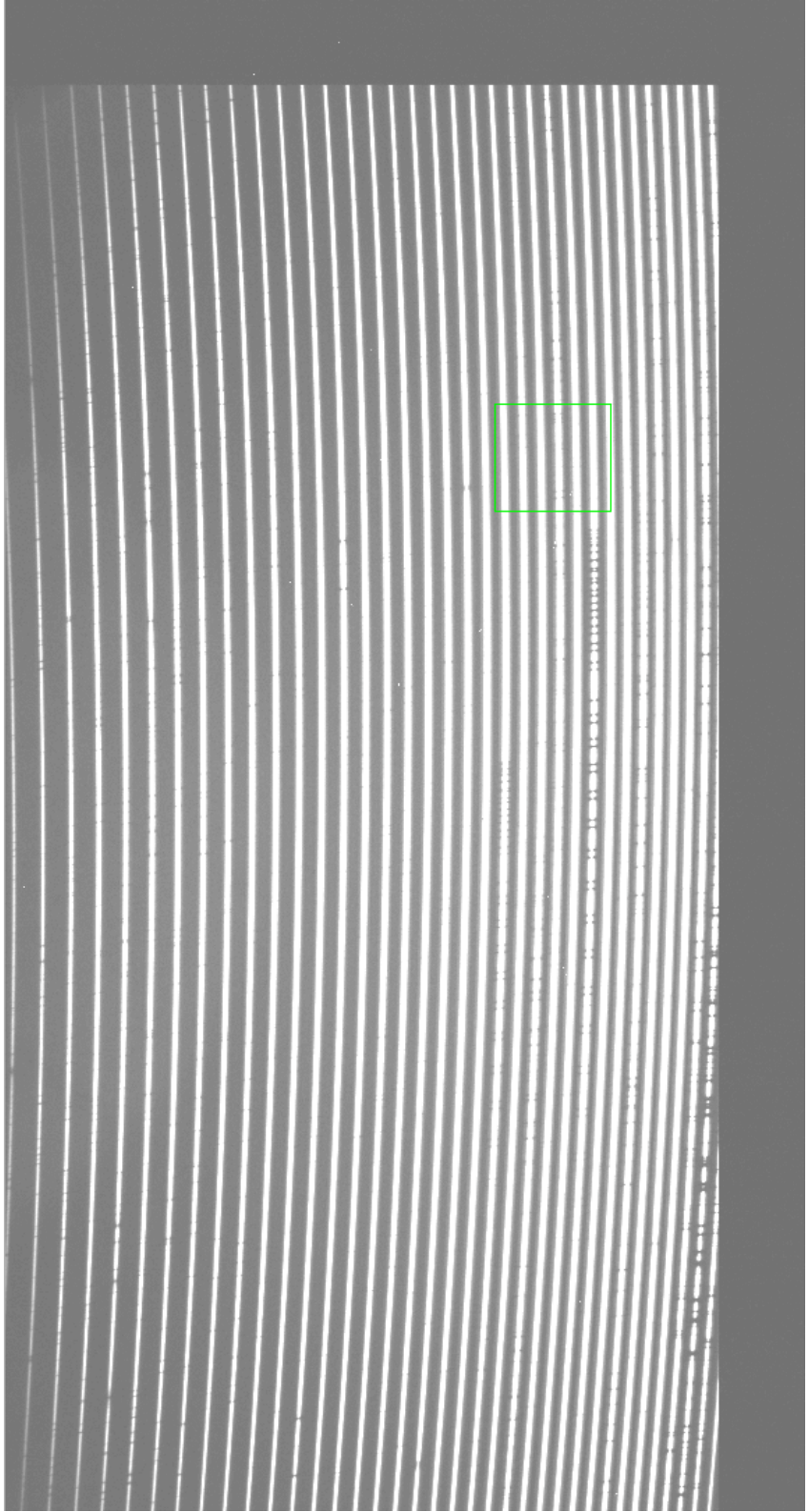

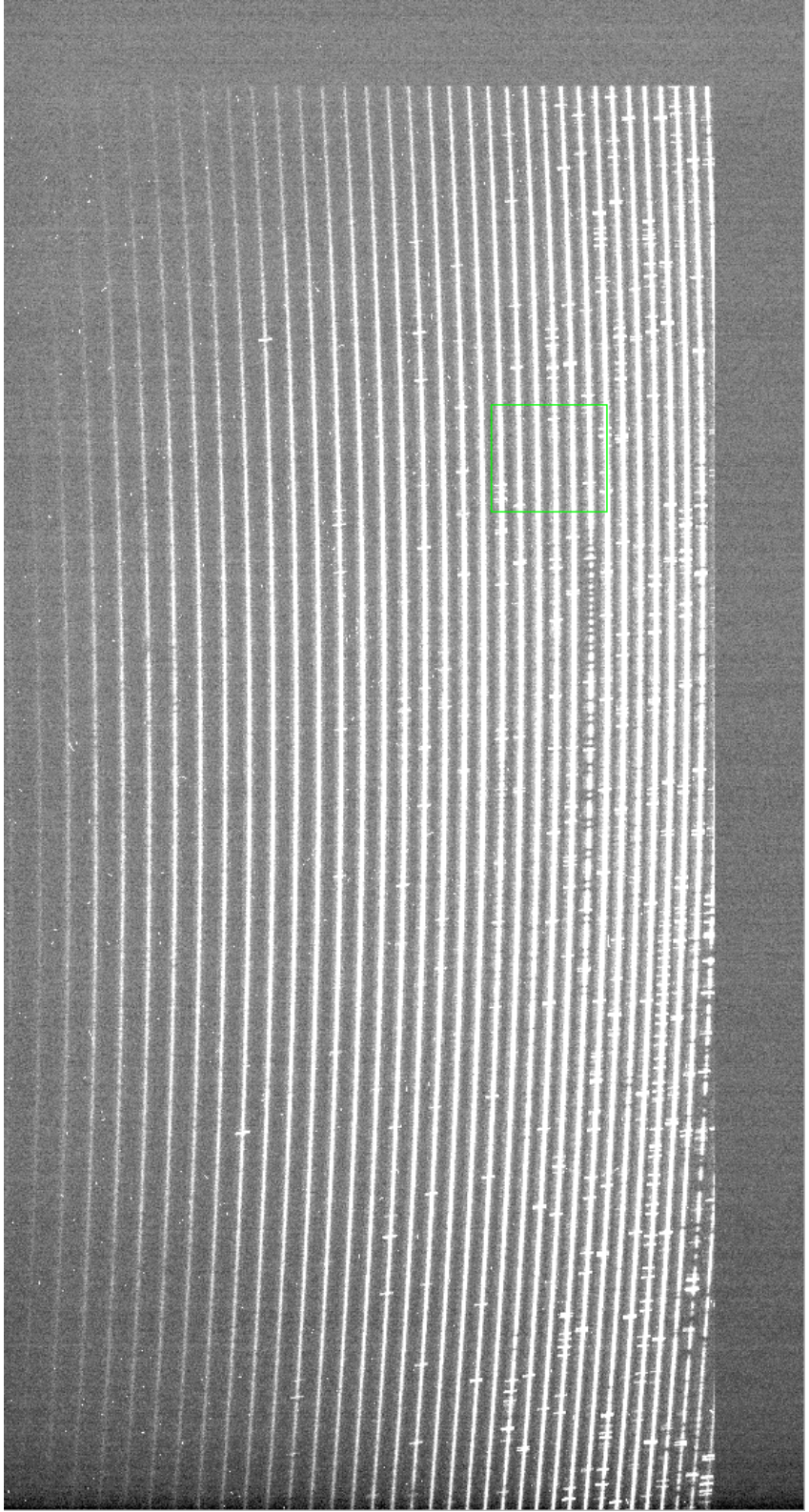

Precision RVs

1 deg T => 100 m/s change

100 hpa => 100 m/s change

Positioning on slit => 100-200 m/s difference

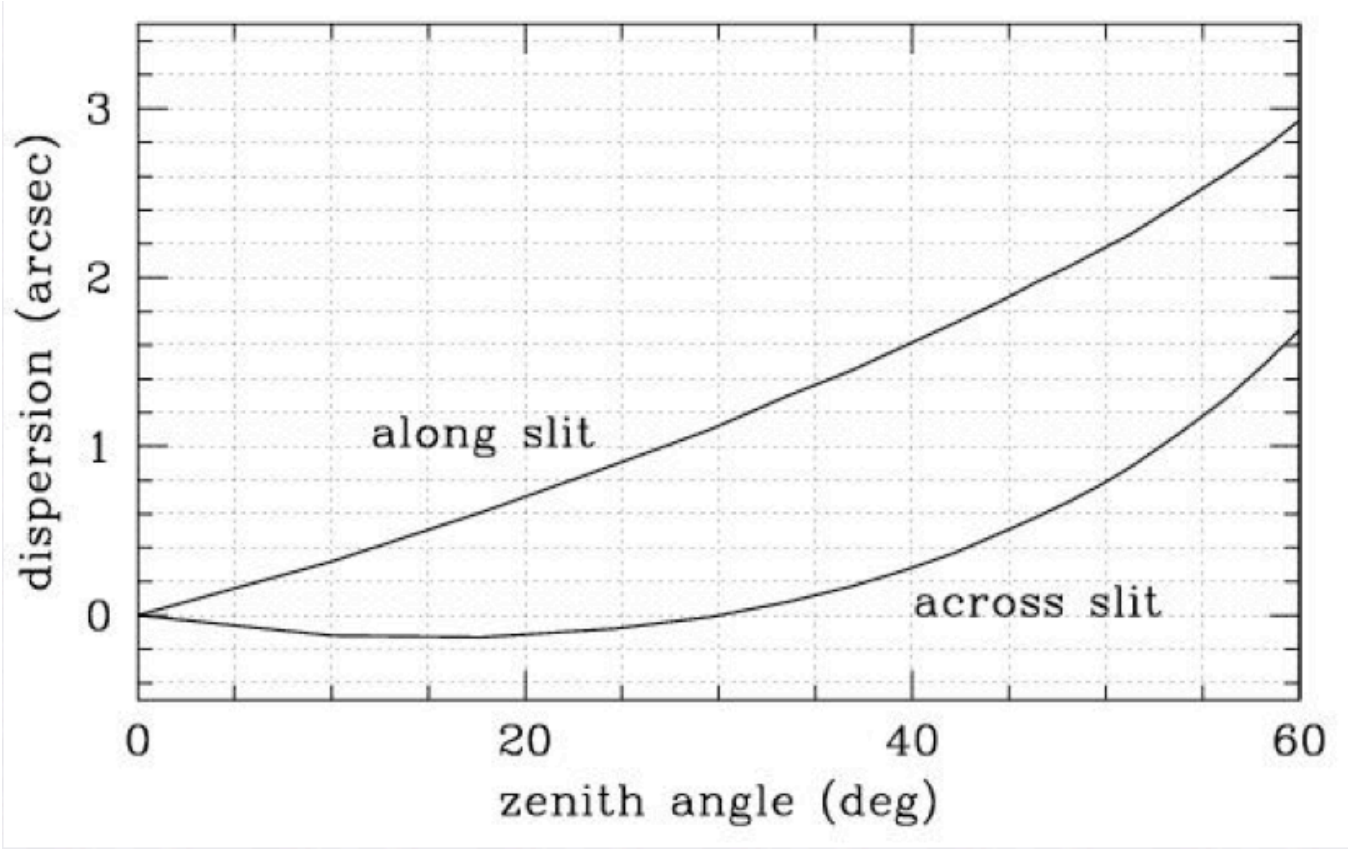

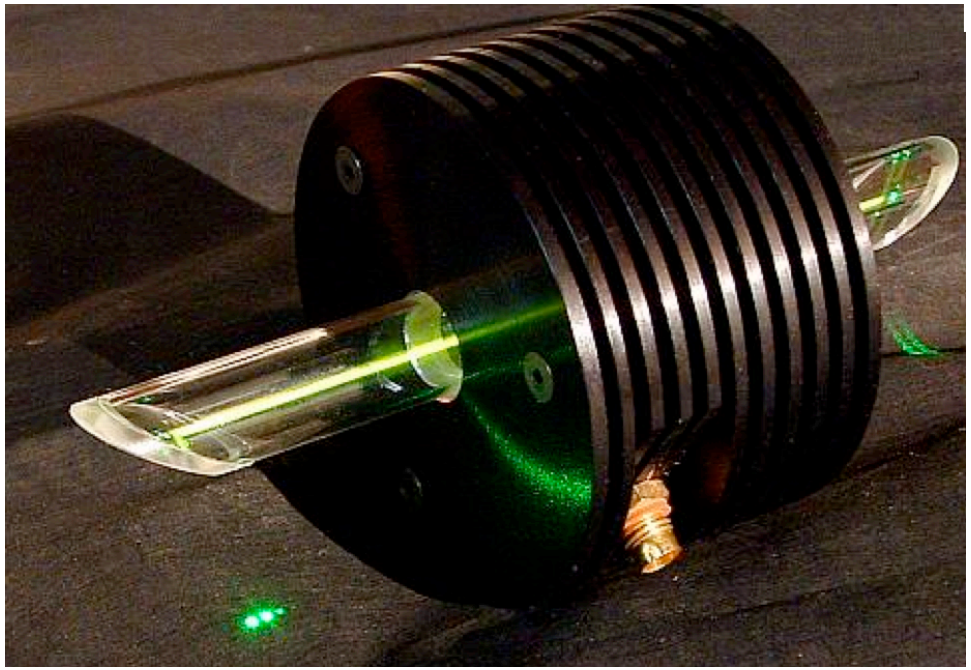

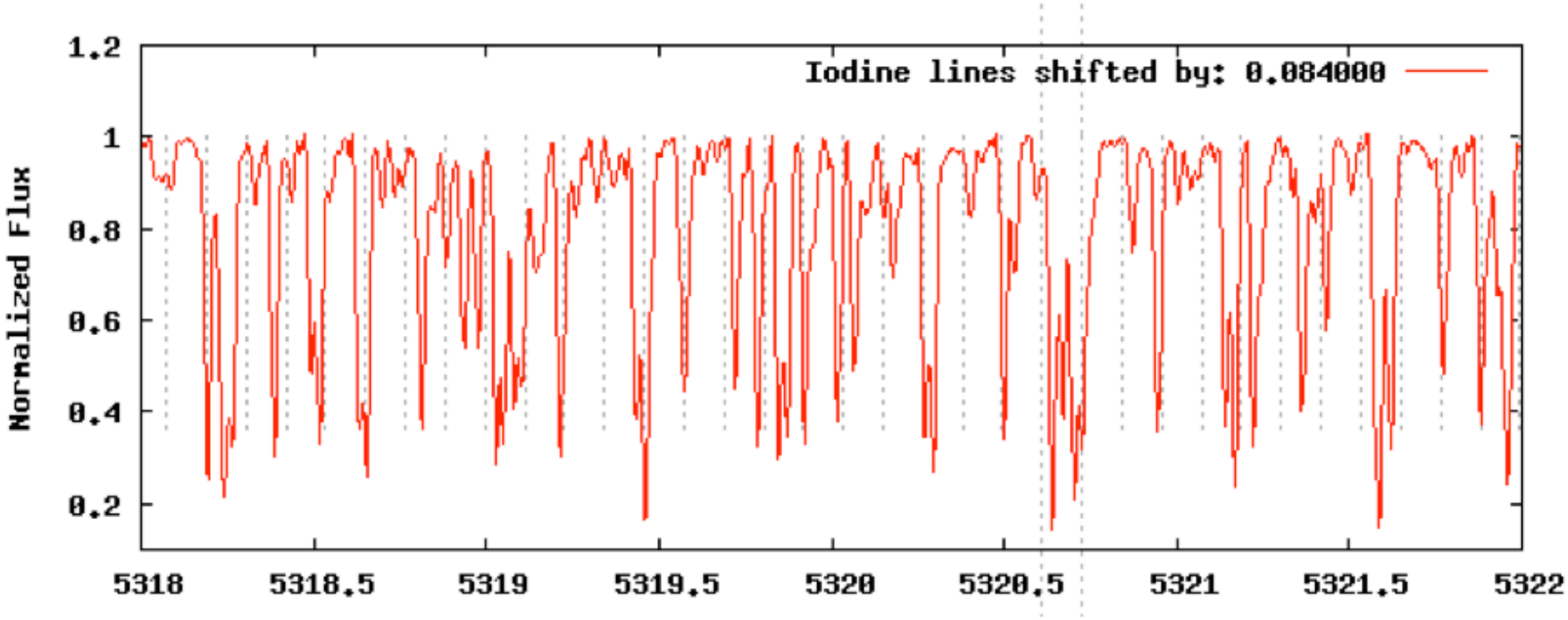
Iodine lines shifted by: 0.084000
Normalized Flux
1.2
1
0.8
0.6
0.4
0.2
5318
5318.5
5319
5319.5
5320
5320.5
5321
5321.5
5322

Iodine cell

High temperature long time needed to heat (1 day)

50 % of the flux eaten by Iodine (big telescopes needed)

Narrow range of spectrum

Deconvolution S/N > 150 required

BUT easy to implement and relatively “cheap”

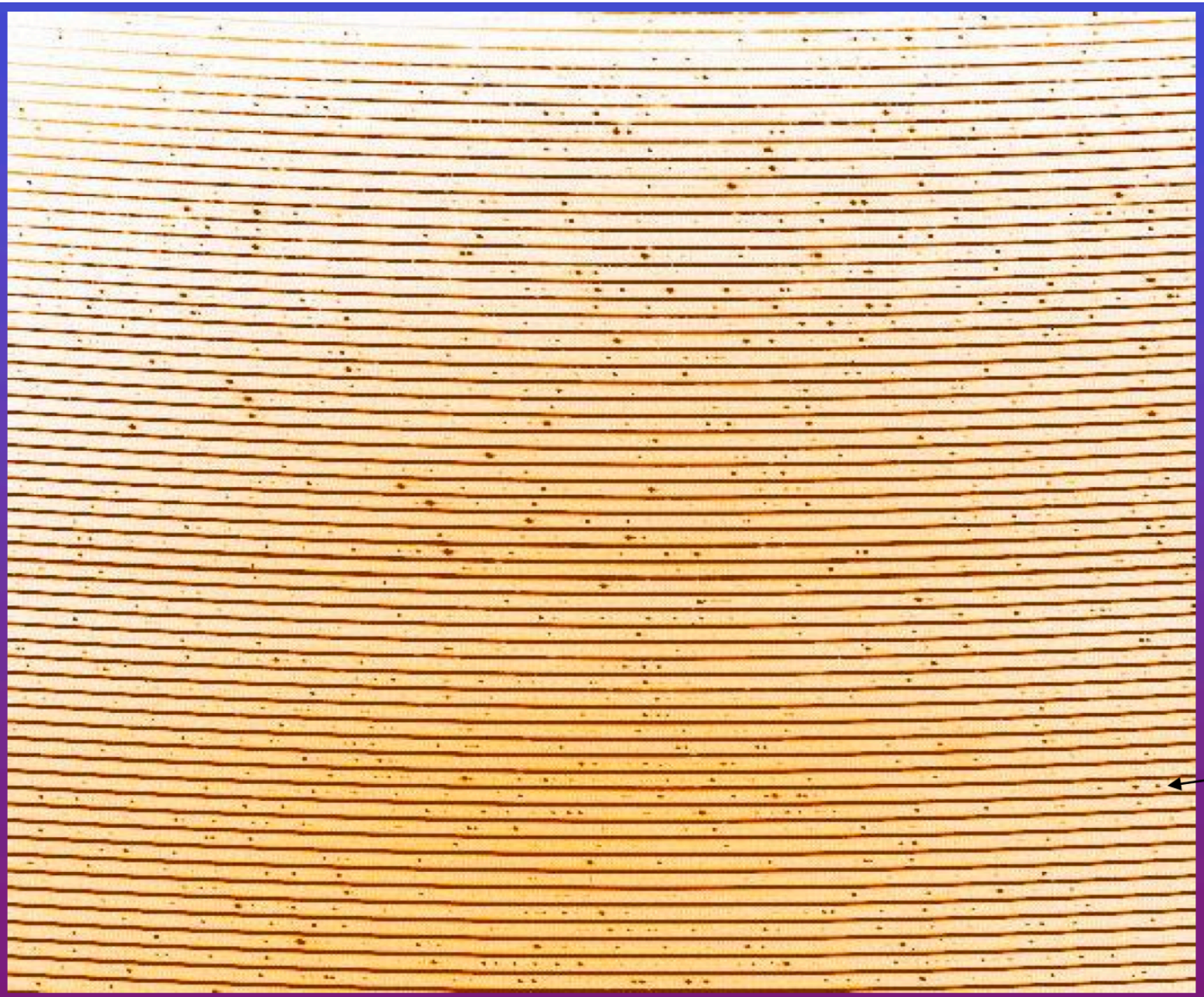

From Mayor 2005

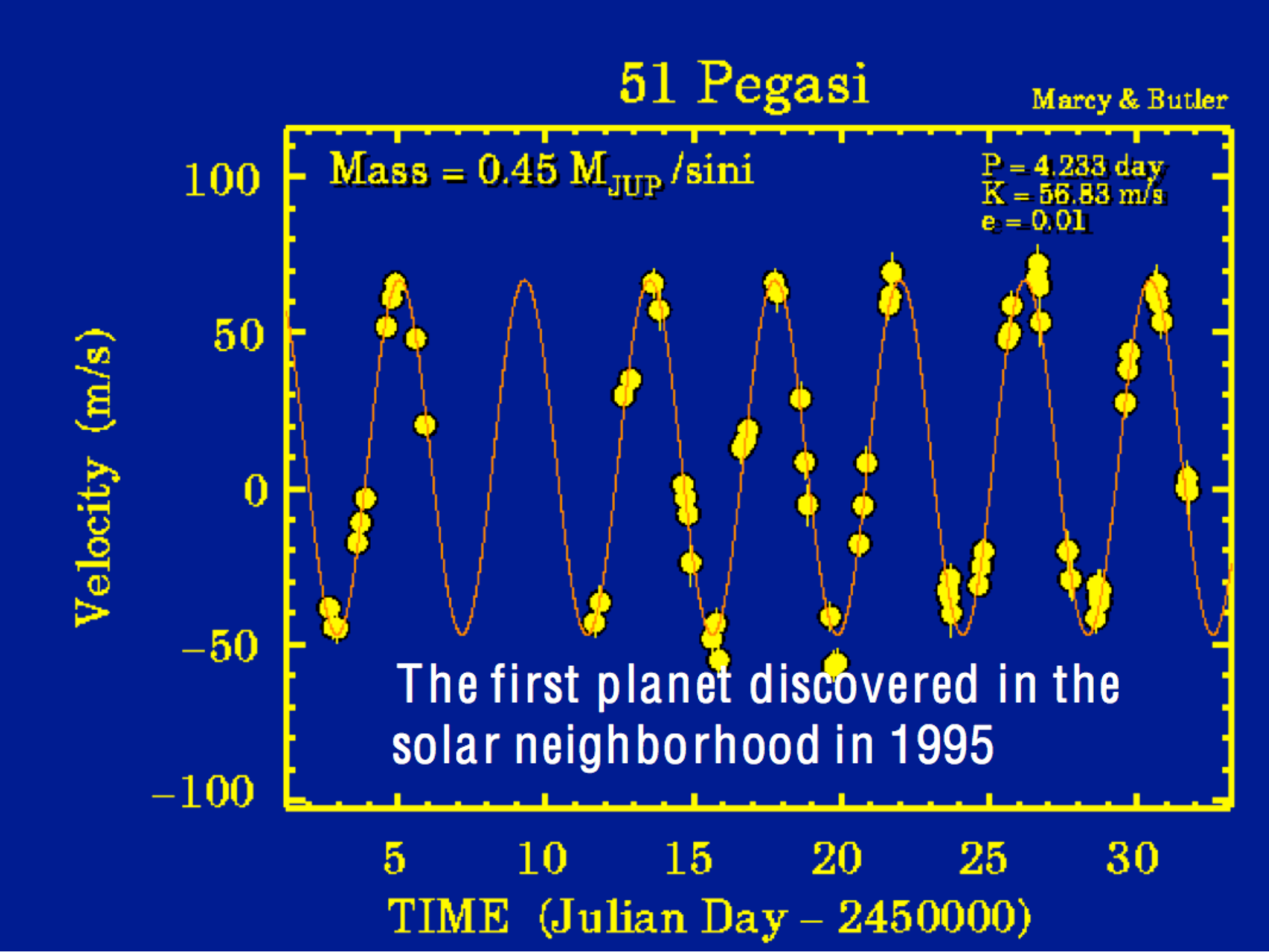
51 Pegasi
Marcy & Butler
Mass = 0.45 M_JUP /sini
P = 4.233 day
K = 56.83 m/s
e = 0.01
100
50
0
−50
−100
Velocity (m/s)
The first planet discovered in the solar neighborhood in 1995
5
10
15
20
25
30
TIME (Julian Day – 2450000)

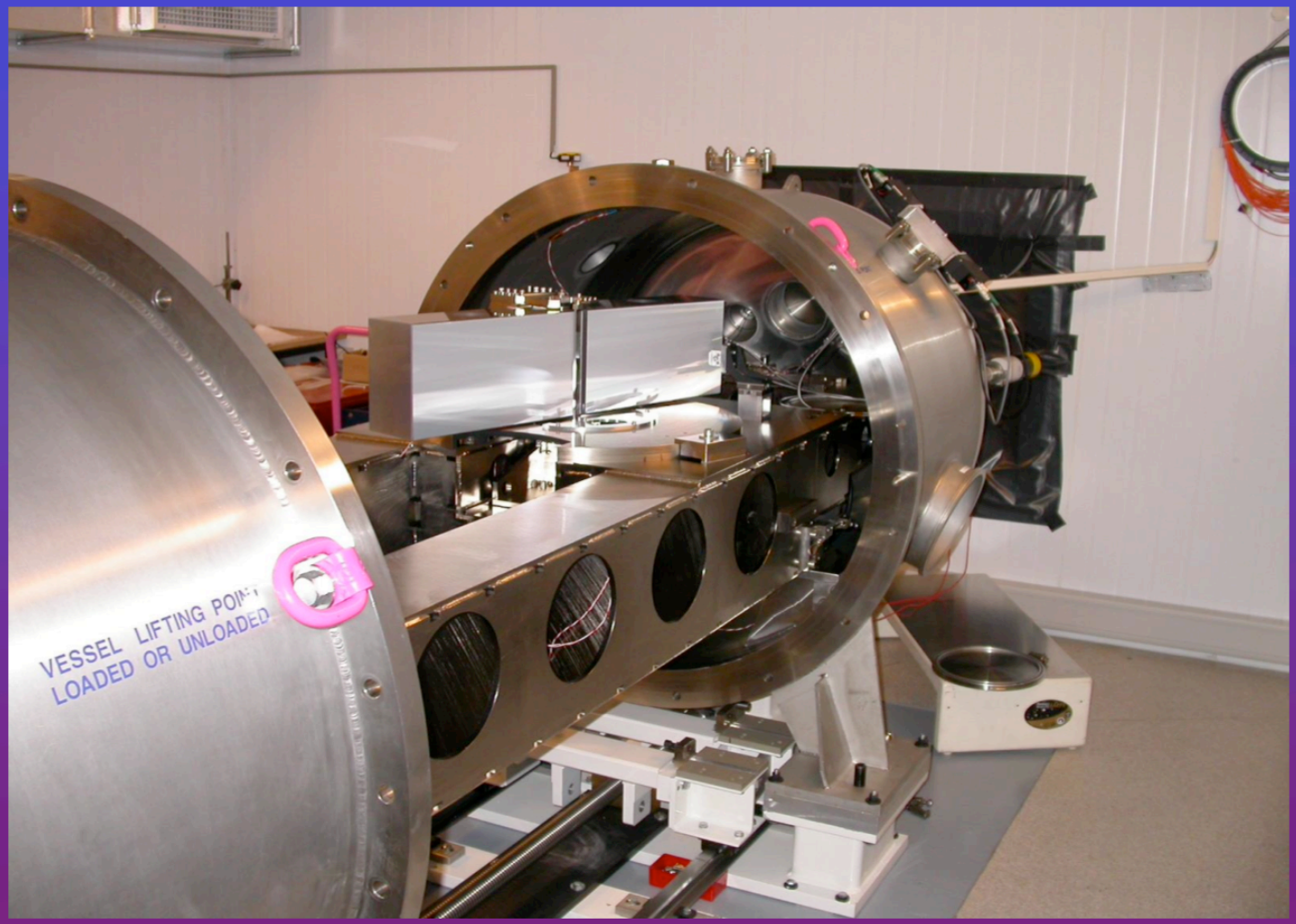

Instrument long term stability:

$\Delta T = 0.01$ K

$\Delta P = 0.01$ mbar

From Mayor 2005

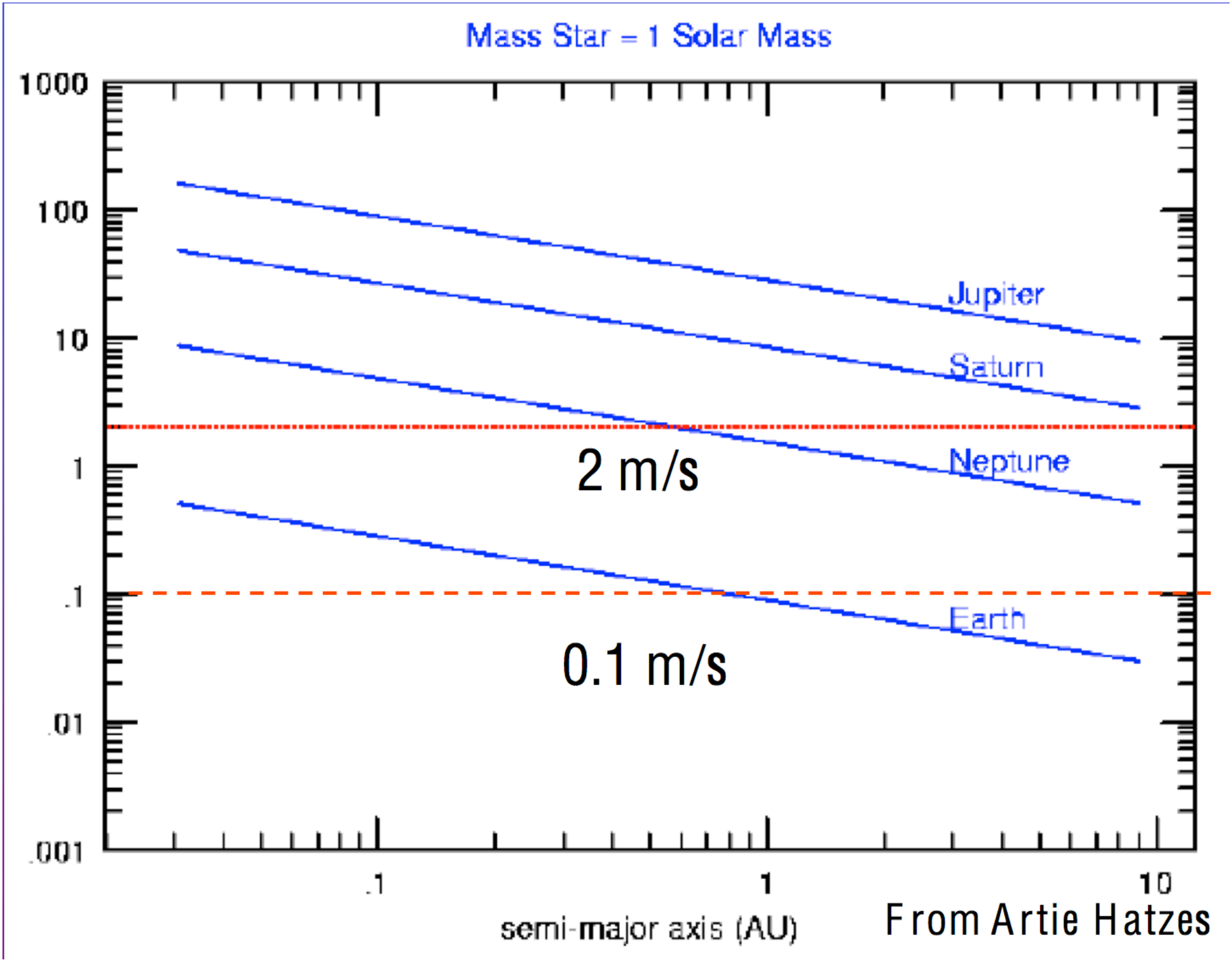
Mass Star = 1 Solar Mass
1000
100
10
1
.1
.01
.001
.1
1
10
Jupiter
Saturn
Neptune
Earth
2 m/s
0.1 m/s
semi-major axis (AU)
From Artie Hatzes

3. ESPRESSO – A NEW-GENERATION SPECTROGRAPH

3.1 Instrument concept

ESPRESSO is a fiber-fed, cross-dispersed, high-resolution, echelle spectrograph. The telescope light is fed to the instrument via a Coudé-Train optical system and fibers. ESPRESSO is located in the Combined-Coudé Laboratory (incoherent focus) where a front-end unit can combine the light from up to 4 Unit Telescopes (UT) of the VLT. The target and sky light enter the instrument through two distinct optical fibers which form the 'slit' of the spectrograph.

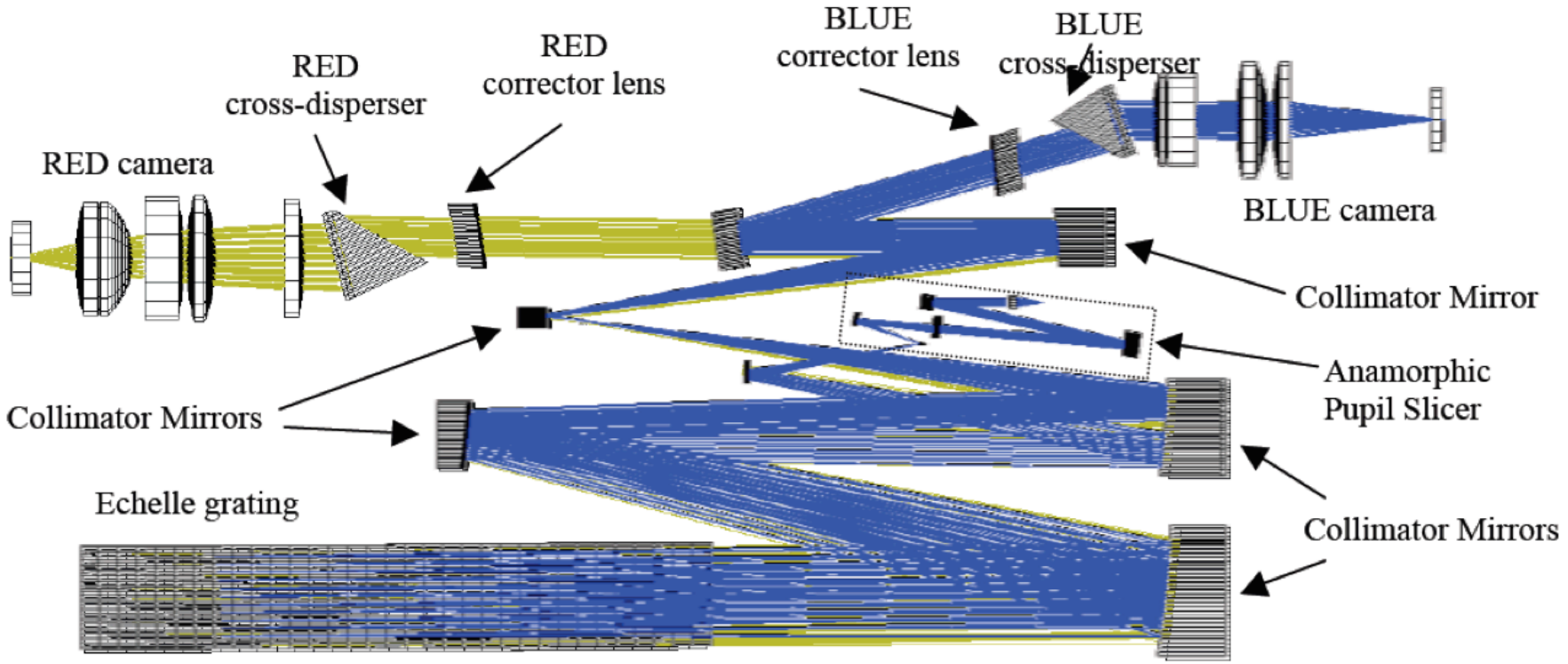

Figure 1. Optical layout of the ESPRESSO spectrograph

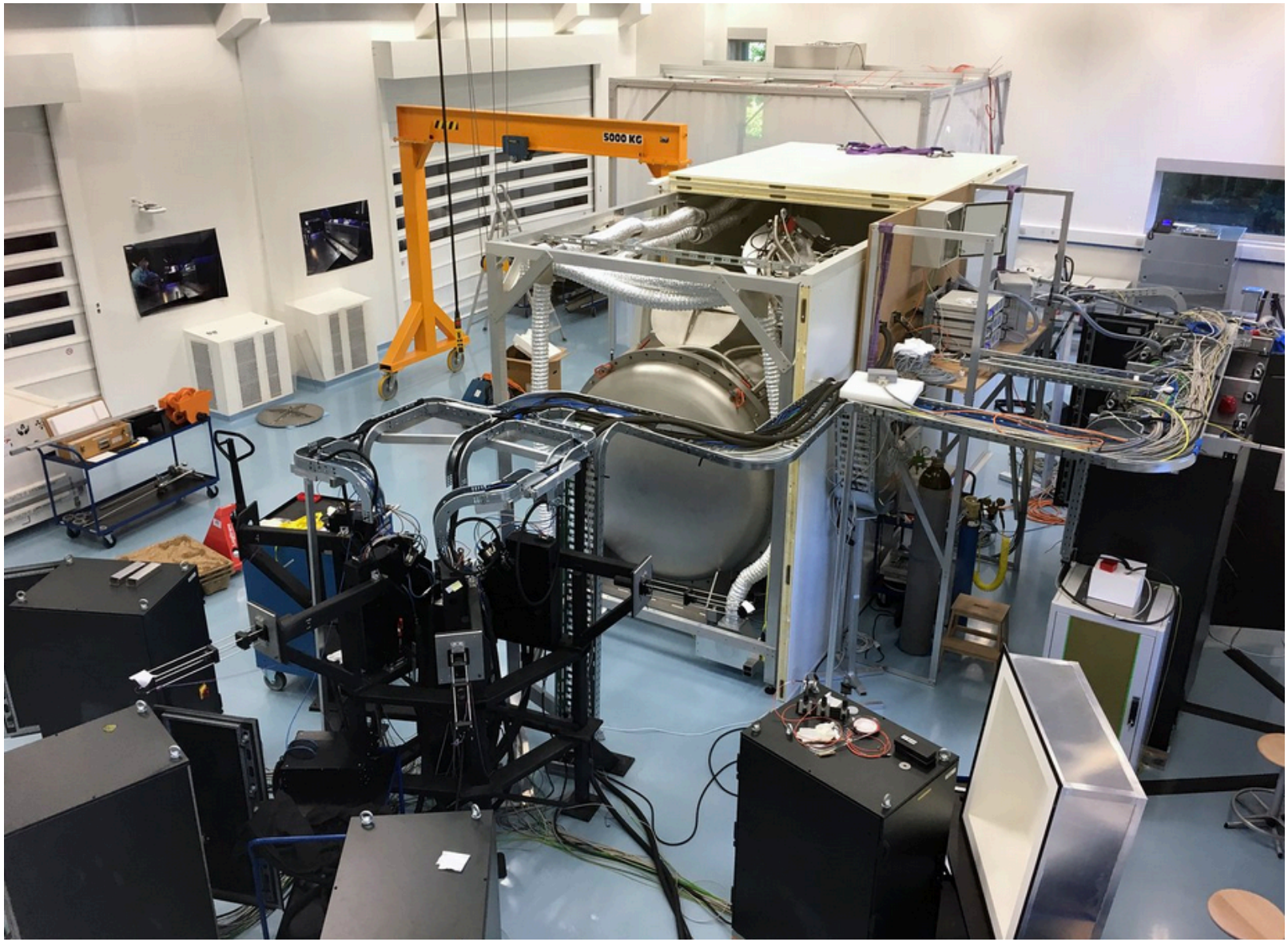
5000 KG

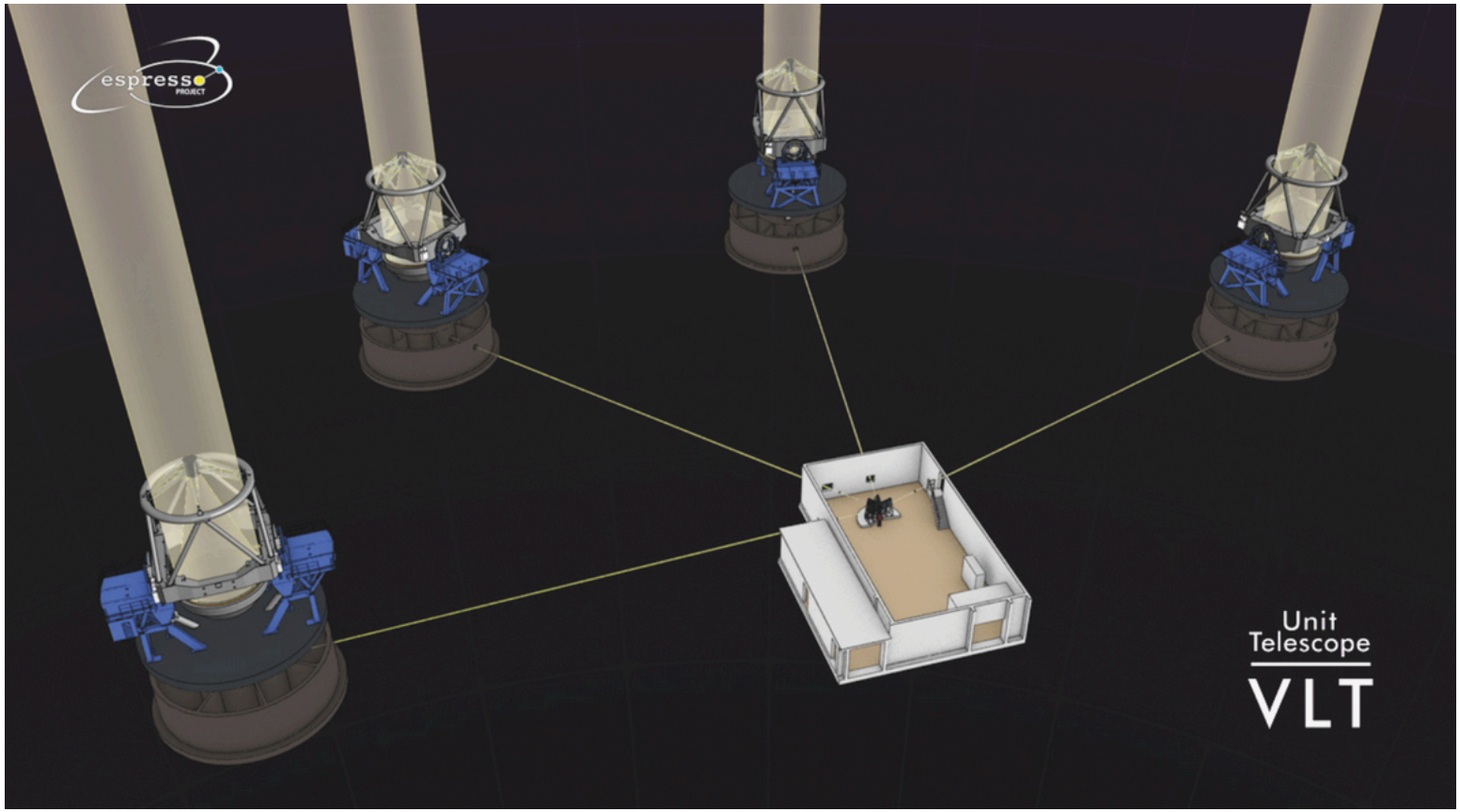
espresso
PROJECT
Unit
Telescope
VLT

	HR (1-UT)	UHR (1-UT)	MR (4-UT)
Wavelength range	380–788 nm	380–788 nm	380–788 nm
Resolving power (median)	140,000	190,000	70,000
Aperture on sky	1".0	0".5	4x1".0
Total efficiency	11%	5%	11%
RV precision (requirement)	< 10 cm/s	< 5 m/s	< 5 m/s
Limiting V-band magnitude*	~17	~16	~20
Binning	1x1, 2x1	1x1	4x2, 8x4
Spectral sampling (average)	4.5 px	2.5 px	5.5 px (binned x2)
Spatial sampling per slice	9.0 (4.5) px	5.0 px	5.5 px (binned x4)
Number of slices	2	2	1

Rocky planets

Stability of physical constants: fine-structure constant (α) and the proton-to-electron mass ratio (μ). A relative variation in α or μ of 1 ppm leads to velocity shifts of about 20 m/s between typical combinations of transitions.

Abundances, blending, rotation

Full list of instrument setups in the FLAMES User manual

Spectrograph	Mode	N. Of Objects	Aperture (")	Resolving Power (*)	Spectral Band [nm] (**)
UVES	Red Arm	8	1.0	47000	200
UVES	Red Arm	7 + 1 calibration	1.0	47000	200
GIRAFFE	MEDUSA buttons	130 (w. sky fibres)	1.2	12000 - 24000	λ/12 to λ/24
GIRAFFE	MEDUSA buttons	130 (w. sky fibres)	1.2	7000	λ/9.5
GIRAFFE	IFU	15 (+15 sky fibres)	2 x 3	19000 - 39000	λ/12 to λ/24
GIRAFFE	IFU	15 (+15 sky fibres)	2 x 3	11000	λ/9.5
GIRAFFE	ARGUS	1	11.5 x 7.3 or 6.6 x 4.2	19000 - 39000	λ/12 to λ/24
GIRAFFE	ARGUS	1	11.5 x 7.3 or 6.6 x 4.2	11000	λ/9.5

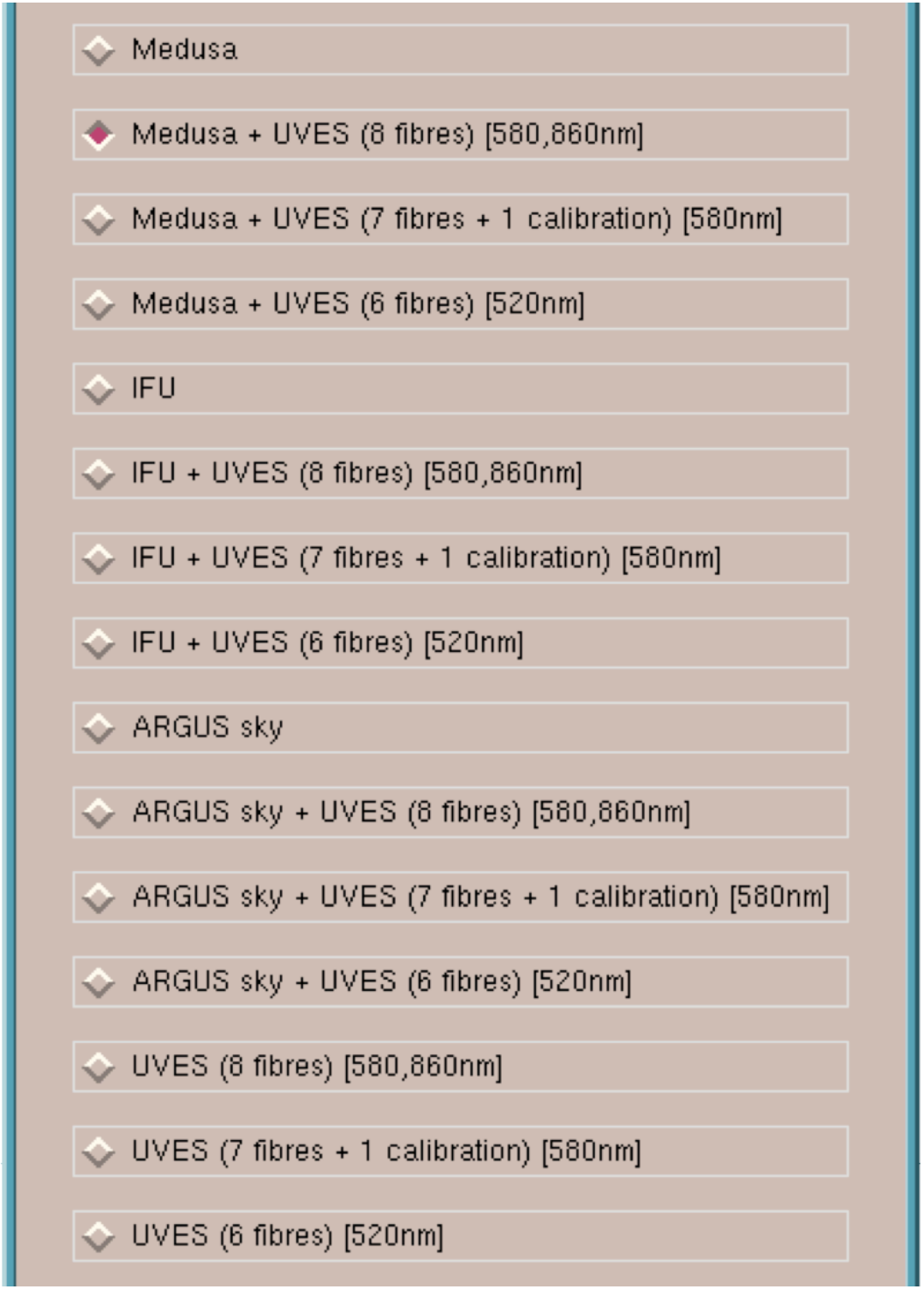
Medusa
Medusa + UVES (8 fibres) [580,860nm]
Medusa + UVES (7 fibres + 1 calibration) [580nm]
Medusa + UVES (6 fibres) [520nm]
IFU
IFU + UVES (8 fibres) [580,860nm]
IFU + UVES (7 fibres + 1 calibration) [580nm]
IFU + UVES (6 fibres) [520nm]
ARGUS sky
ARGUS sky + UVES (8 fibres) [580,860nm]
ARGUS sky + UVES (7 fibres + 1 calibration) [580nm]
ARGUS sky + UVES (6 fibres) [520nm]
UVES (8 fibres) [580,860nm]
UVES (7 fibres + 1 calibration) [580nm]
UVES (6 fibres) [520nm]

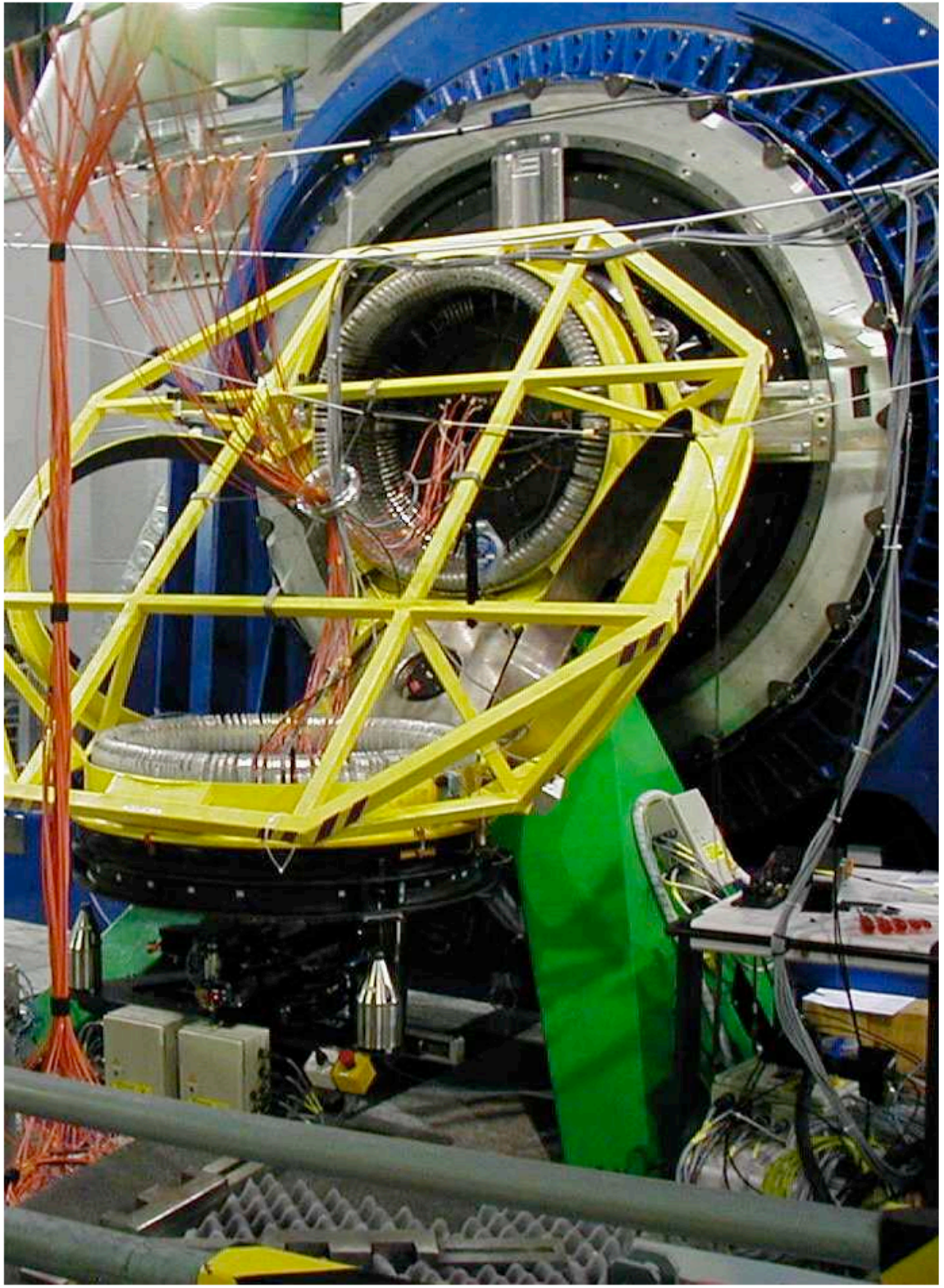

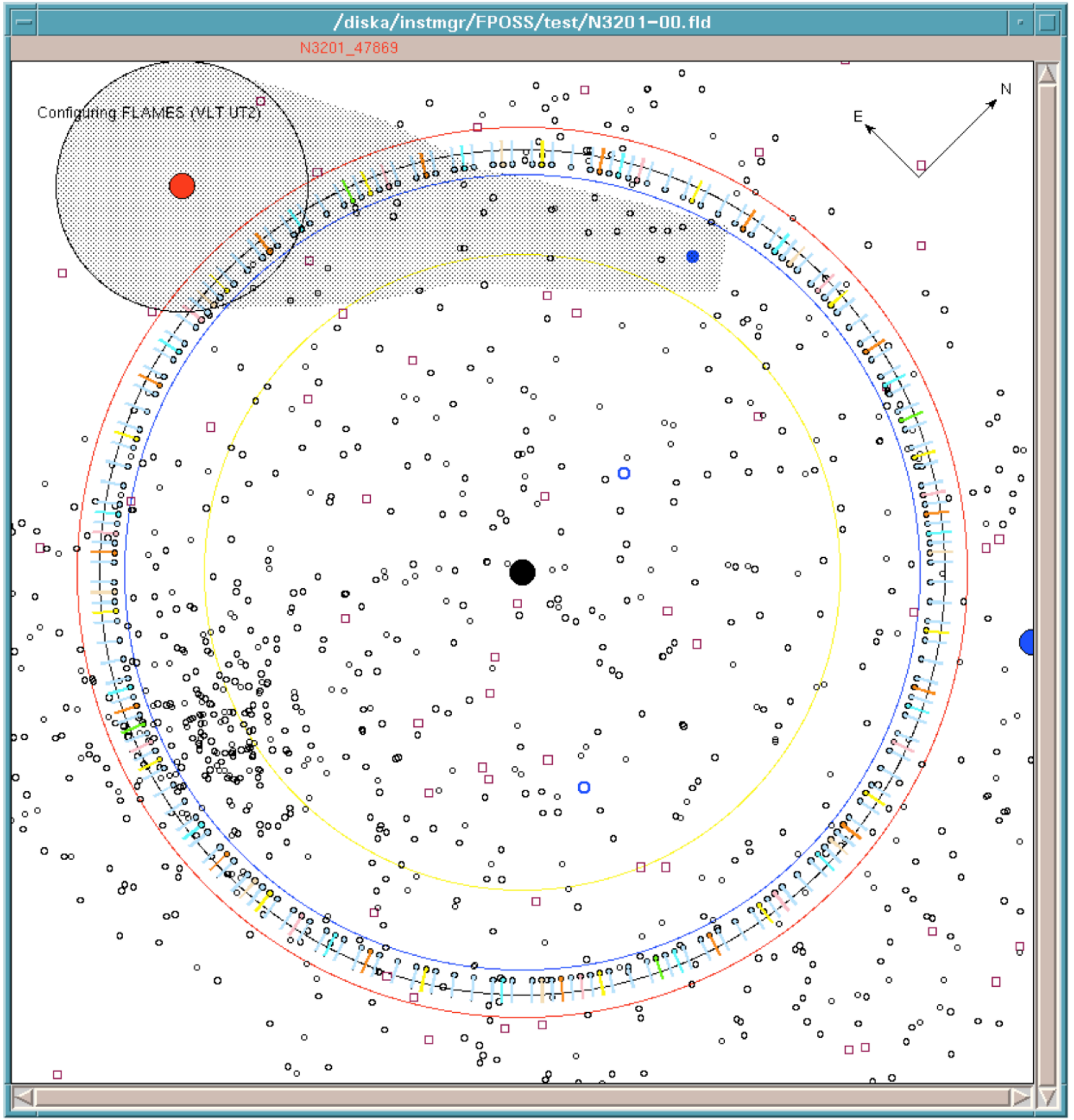
/diska/instmgr/FPOSS/test/N3201-00.fld
N3201_47869
Configuring FLAMES (VLT UT2)
N
E

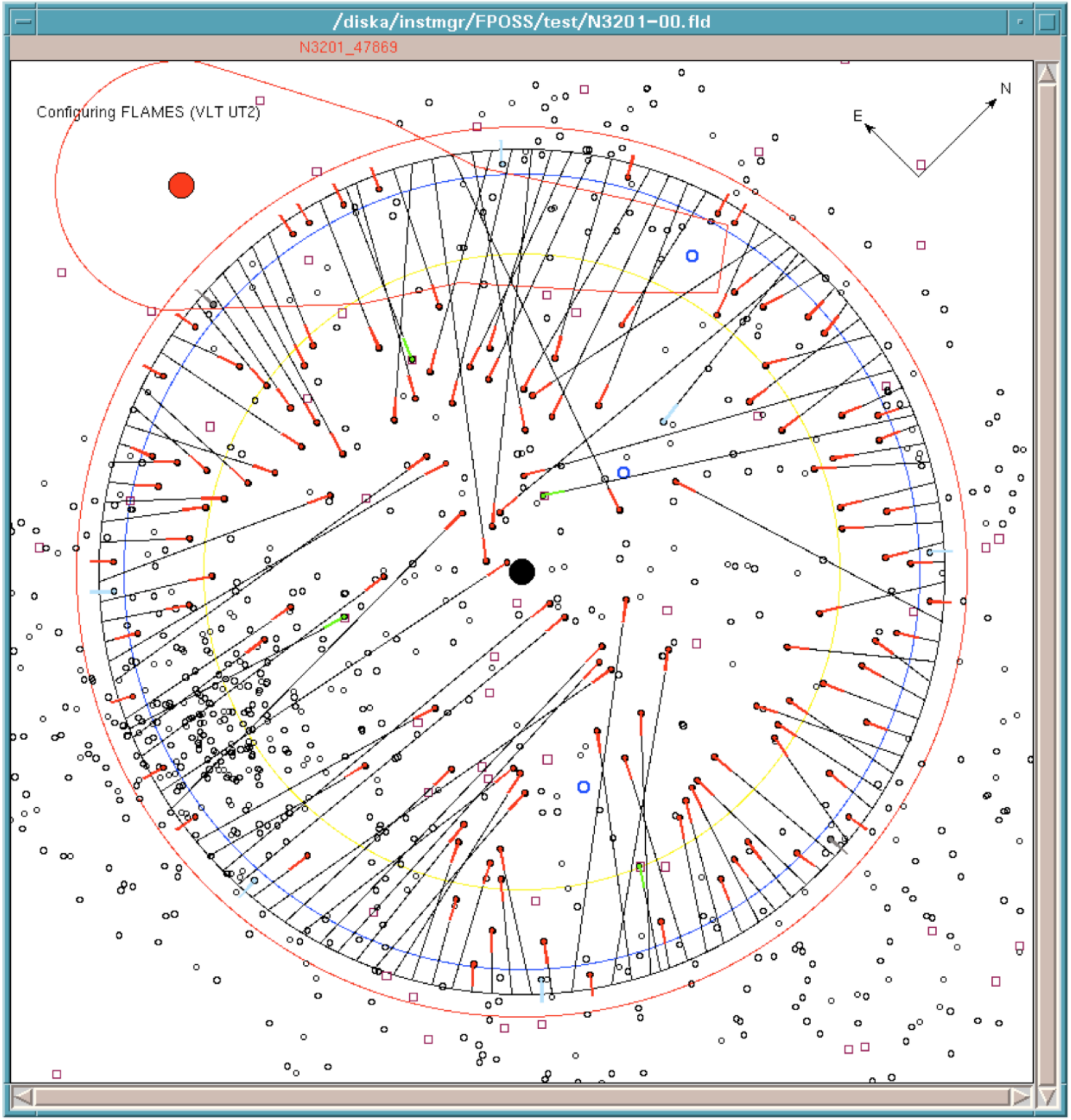
/diska/instmgr/FPOSS/test/N3201-00.fld
N3201_47869
Configuring FLAMES (VLT UT2)
N
E

4MOST

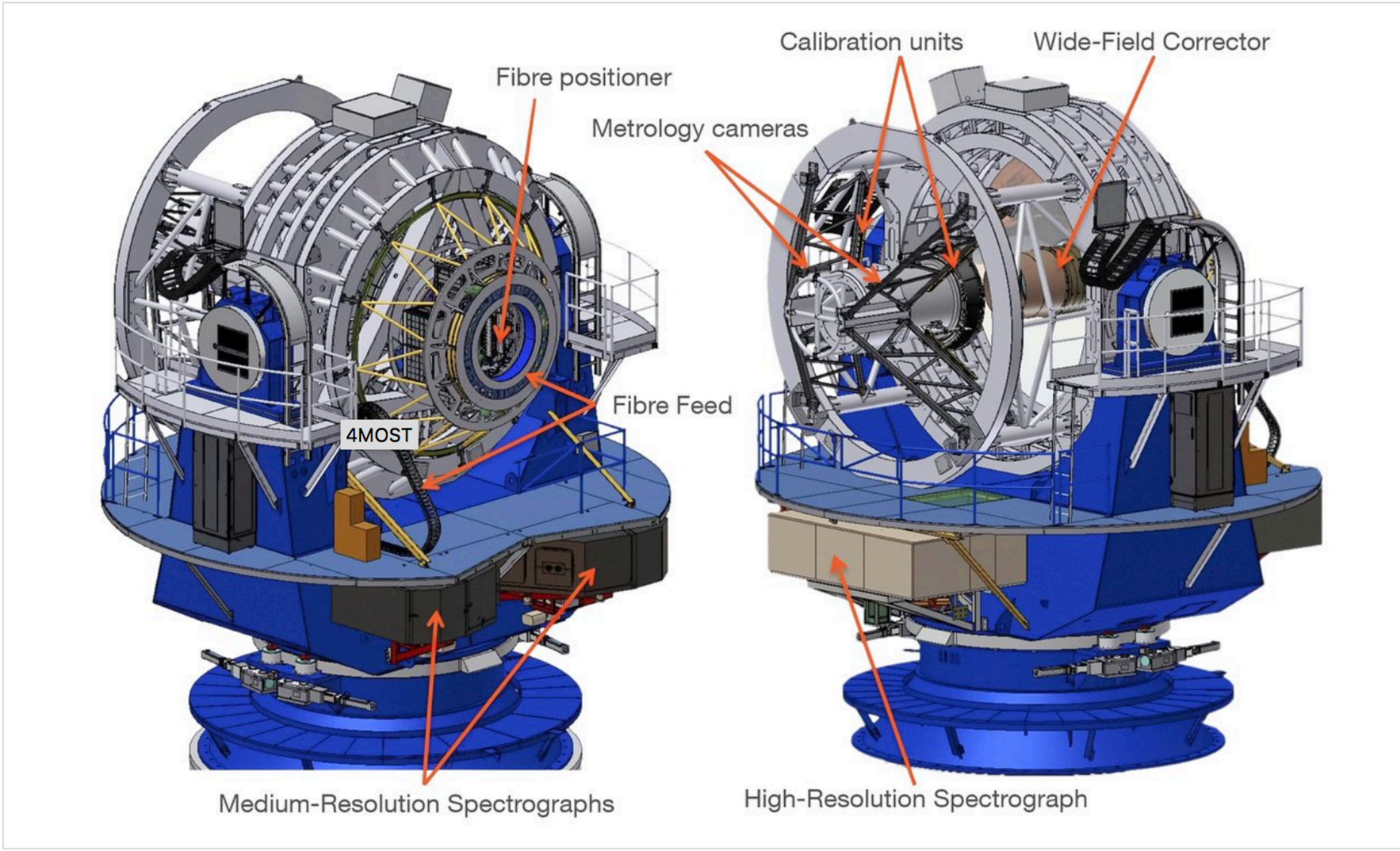

2400 fibers 390-950 nm expected in 2022

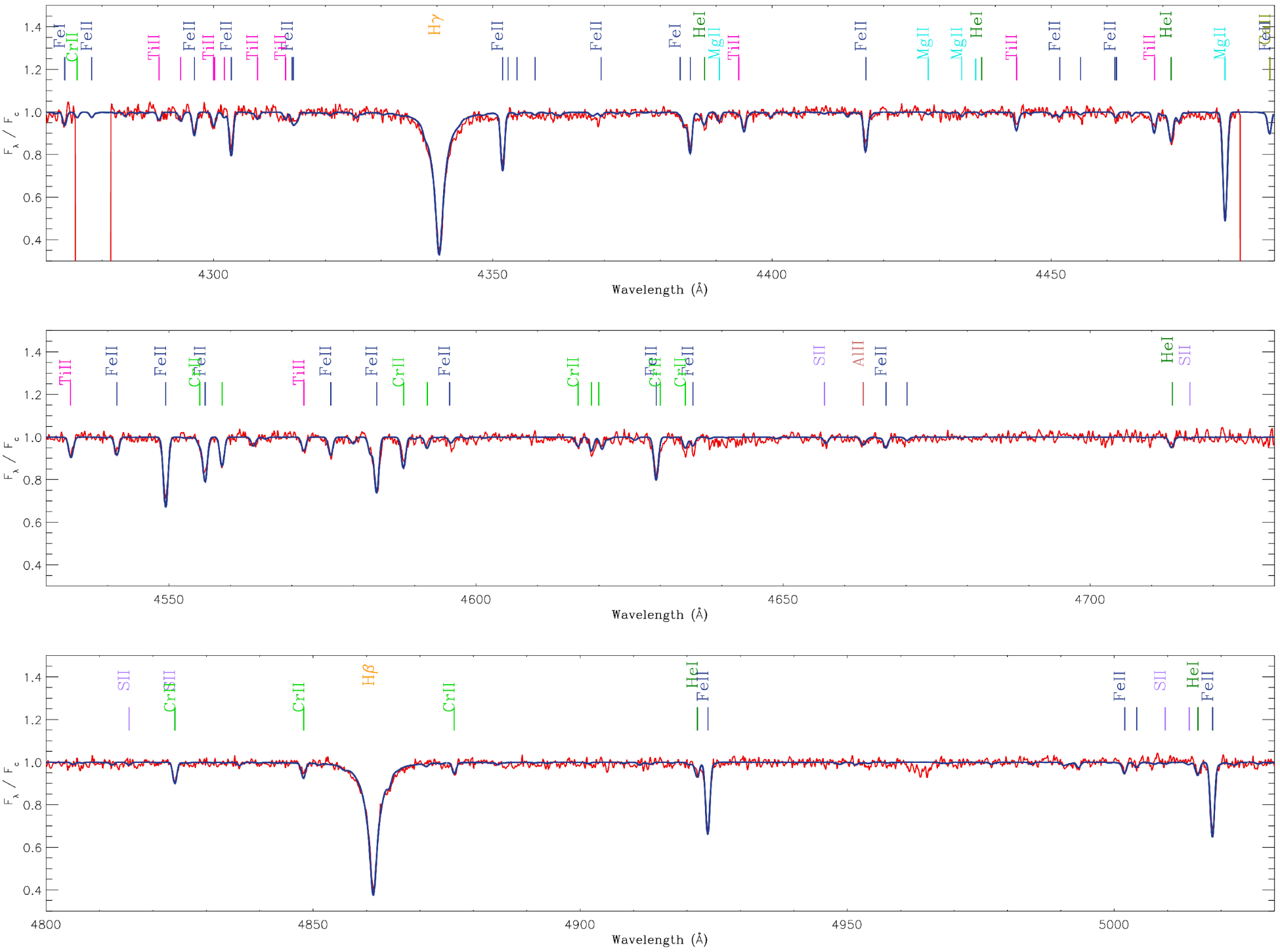
FeI
CrII
FeII
TiII
FeII
TiII
FeII
TiII
TiII
FeII
Hγ
FeII
FeII
FeI
HeI
MgII
TiII
FeII
MgII
MgII
HeI
TiII
FeII
FeII
TiII
HeI
MgII
CaII
CaII
F_λ / F_c
1.4
1.2
1.0
0.8
0.6
0.4
4300
4350
4400
4450
Wavelength (Å)
TiII
FeII
FeII
CrII
FeII
TiII
FeII
FeII
CrII
FeII
CrII
CrII
FeII
CrII
FeII
SII
AlII
FeII
HeI
SII
4550
4600
4650
4700
Wavelength (Å)
SII
CrII
FeII
CrII
Hβ
CrII
HeI
FeII
FeII
SII
HeI
FeII
4800
4850
4900
4950
5000
Wavelength (Å)

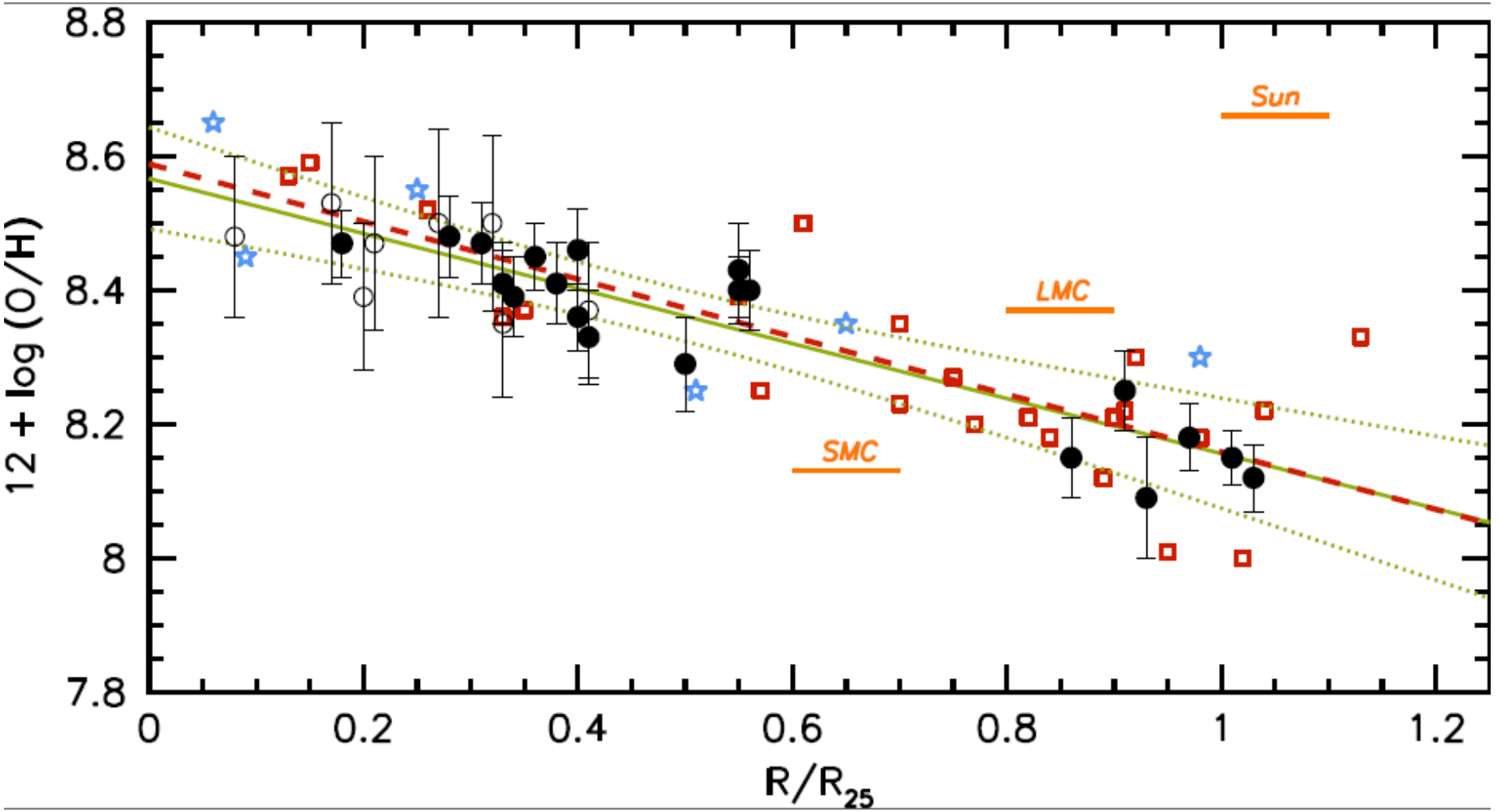
8.8
8.6
8.4
8.2
8
7.8
12 + log (O/H)
0
0.2
0.4
0.6
0.8
1
1.2
R/R25
Sun
LMC
SMC

Flux weighted Gravity – Luminosity Reationship (FGLR)

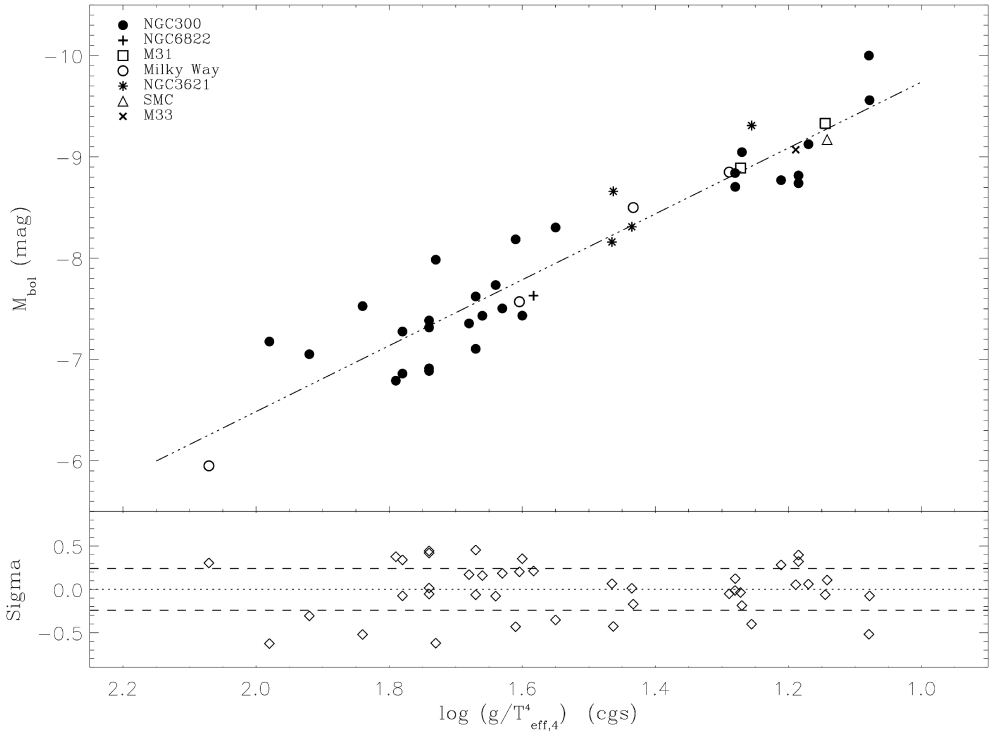

L,M ~ const.

$$M \sim g \times R^2 \sim L \times (g/T^4) = \text{const.}$$

const.

$$\rightarrow L \sim M^x \sim L^x (g/T^4)^x,\ x \sim 3$$

$$\rightarrow L^{1-x} \sim (g/T^4)^x$$

or with $M_{bol} \sim -2.5 \log L$

$$M_{bol} = a \log(g/T^4) + b \qquad \text{(FGLR)}$$

$$a = 2.5\, x/(1-x) \sim 3.75$$

OGLE-051019.64-685812.3

(Pietrzynski et al. 2009, ApJ, 697, 862)